Brunner Thomas (Orcid ID: 0000-0002-1594-4712)



# Immune escape of colorectal tumors via local LRH-1/Cyp11b1-mediated synthesis of immunosuppressive glucocorticoids

**Running Title: Colorectal tumors and glucocorticoids**

Asma Ahmed[1,2,11], Cindy Reinhold[1], Eileen Breunig[1], Truong San Phan[1], Lea Dietrich[1], Feodora Kostadinova[1,12], Corinne Urwyler[3], Verena M. Merk[1], Mario Noti[4,13], Israel Toja da Silva[5,6], Konstantin Bode[1], Fatima Nahle[1], Anna Pia Plazzo[1], Julia Koerner[7], Regula Stuber[4], Constantin Menche[8,9], Eva Karamitopoulou[4], Henner F. Farin[8,9], Kenneth J. Gollob[5,6,10], Thomas Brunner[1,*]

[1]Division of Biochemical Pharmacology, Department of Biology, University of Konstanz, Konstanz, Germany

[2]Department of Pharmacology, Faculty of Medicine, University of Khartoum, Khartoum, Sudan

[3]Institute of Molecular Health Sciences, Department of Biology, Swiss Federal Institute of Technology (ETH) Zurich, Zurich, Switzerland

[4]Institute of Pathology, University of Bern, Bern, Switzerland

[5] International Research Center, A.C. Camargo Cancer Center, São Paulo, SP, Brazil

[6]National Institute for Science and Technology - Oncogenomics and Therapeutic Innovation (INCT-INOTE), São Paulo, SP, Brazil

[7]Division of Immunology, Department of Biology, University of Konstanz, Konstanz, Germany

[8]Georg-Speyer-Haus, Institute for Tumor Biology and Experimental Therapy, Frankfurt am Main, Germany

[9]Frankfurt Cancer Institute, Goethe University, Frankfurt am Main, Germany

[10]Albert Einstein Israelite Hospital, São Paulo, SP, Brazil

[11]present address: Cancer Research UK Beatson Institute, Bearsden G611BD, UK

[12]present address: LHO Laboratory for Hematology and Oncology, 68161 Mannheim, Germany

[13]present address: Société des Produits Nestlé, Nestlé Research, 1000 Lausanne, Switzerland

This article has been accepted for publication and undergone full peer review but has not been through the copyediting, typesetting, pagination and proofreading process which may lead to differences between this version and the Version of Record. Please cite this article as doi: 10.1002/1878-0261.13414

* Corresponding author: Thomas Brunner, Biochemical Pharmacology, Dept. Biology, University of Konstanz, Universitätsstrasse 10, 78457 Konstanz, Germany, thomas.brunner@uni-konstanz.de

**Keywords**

Colorectal cancer, CYP11B1, glucocorticoids, tumor immune escape, immune checkpoint, Liver Receptor Homolog-1 (NR5A2)

**Abbreviations**

AOM, azoxymethane; Ccnd1, cyclin D1; Ccne1, cyclin E1; CTLA-4, cytotoxic T lymphocyte-associated antigen 4; CYP, cytochrome p450; CYP11B1, 11β-hydroxylase; DSS, dextran sodium sulfate; IL, interleukin; LRH-1, Liver Receptor Homolog-1 (NR5A2); MHC, major histocompatibility complex; NK, natural killer; PD1, programmed death 1; SHP, Small Heterodimer Partner (NR0B2); SF-1, Steroidogenic Factor-1 (NR5A1); TGFβ, transforming growth factor β; $T_{reg}$, regulatory T cells; TNF, tumor necrosis factor

**Abstract**

Control of tumor development and growth by the immune system critically defines patient fate and survival. What regulates the escape of colorectal tumors from destruction by the immune system is currently unclear. Here, we investigated the role of intestinal synthesis of glucocorticoids in the tumor development during inflammation-induced mouse model of colorectal cancer. We demonstrate that the local synthesis of immunoregulatory glucocorticoids has dual roles in the regulation of intestinal inflammation and tumor development. In the inflammation phase LRH-1/Nr5A2-regulated and Cyp11b1-mediated intestinal glucocorticoid synthesis prevents tumor development and growth. In established tumors, however, tumor-autonomous Cyp11b1-mediated glucocorticoid synthesis suppresses anti-tumor immune responses and promotes immune escape. Transplantation of glucocorticoid synthesis-proficient colorectal tumor organoids into immunocompetent recipient mice resulted in rapid tumor growth, whereas transplantation of Cyp11b1-deleted and glucocorticoid synthesis-deficient tumor organoids was characterized by reduced tumor growth and increased immune cell infiltration. In human colorectal tumors, high expression of steroidogenic enzymes correlated with the expression of other immune checkpoints and suppressive cytokines, and negatively correlated with overall patients' survival. Thus, LRH-1-regulated tumor-specific glucocorticoid synthesis contributes to tumor immune escape and represents a novel potential therapeutic target.

## Introduction

The control of tumor development and growth by the immune system has been first suggested more than 50 years ago [1], however, its physiological relevance has been questioned for decades. Though many tumors express tumor-specific or tumor-associated antigens, and tumor patients have tumor-specific T cells, it has been unclear if and how much these immune effector cells contribute to the control of tumor growth. More recent studies, however, strongly support the idea that immune surveillance critically limits tumor development and growth. In colorectal tumor patients, infiltration of tumors with effector memory $CD8^+$ T cells has been associated with increased patient survival [2, 3]. This has led to the development of a so-called “immunoscore”, which stratifies colorectal tumor patients based on the extent and quality of immune cell infiltrates (reviewed in [4]). The tumor microenvironment is, however, not only populated by tumor-controlling cytotoxic T cells, but also by other types of immune cells, which may even support tumor development by either suppressing the immune response, or by promoting tumor vascularization and thereby tumor growth. Colorectal tumors are often associated with increased numbers of $FoxP3^+$ regulatory T cells ($T_{reg}$), which may limit protective immune surveillance [5]. Similarly, tumor-associated macrophages are frequently present in the microenvironment of colorectal tumors. While pro-inflammatory M1-like macrophages are correlated with increased survival, the presence of anti-inflammatory M2-like macrophages is associated with poor prognosis (reviewed in [6]).

These findings suggest that the ability of tumors to condition their microenvironment may largely determine whether or not the immune system is able to control tumor growth and metastases. Thus, tumor-derived factors, which limit the infiltration, activation or even survival of tumor-specific T lymphocytes, likely substantially support tumor growth and immune evasion. The “tool kit” of cancer cells in this regard is rather extensive. Tumor cells downregulate MHC class I to prevent recognition by cytotoxic T cells [7], release TGFβ to suppress their activation [8], or express cytotoxic effector molecules usually restricted to cytotoxic lymphocytes, e.g. Fas (CD95) ligand, and thereby induce apoptosis in tumor-infiltrating immune cells [9, 10]. Tumor cells also highjack regulatory mechanisms, which usually contribute to the regulation of immune tolerance, and thereby prevent excessive tissue damage. The inhibitory receptors cytotoxic T lymphocyte-associated antigen 4 (CTLA-4) and programmed death 1 (PD1) generally interact with their cognate ligands CD80 and PD1L, respectively, on antigen-presenting cells. Balanced activation of these inhibitory receptors critically contributes to the maintenance of immune homeostasis, as evidenced by the development of autoimmune disease in CTLA-4- and PD1-deficient mice. The same

inhibitory receptors, however, also prevent activation of tumor-specific T cells. This is why anti-PD1L and anti-CTLA-4 antibodies have a therapeutic effect in tumor patients, in particular when applied in combination with cell death-promoting agents, likely by enhancing immunological cell death [11].

Yet, not all patients respond to immune checkpoint inhibitors, i.e. anti-PD-L1 and anti-CTLA-4 antibodies. This suggest that different immunoregulatory mechanisms exist, which prevent destruction of tumors by the immune system. Glucocorticoids are steroid hormones with potent immunosuppressive activities. Since their discoveries in the 1950s they could not be missed in the treatment of numerous devastating inflammatory and autoimmune diseases. Endogenous glucocorticoids are primarily produced in the adrenal glands in response to emotional, physical and inflammatory stress. In the last two decades, various alternative sources of glucocorticoids, such as thymus, skin, lung, vasculature and intestine, have been discovered (reviewed in [12-14]). In the intestine, we identified the intestinal crypts as the relevant source of glucocorticoids [15]. Interestingly, the regulation of the intestinal and adrenal glucocorticoid synthesis differs substantially. While in the adrenal glands steroidogenesis is under the transcriptional control of the nuclear receptor Steroidogenic Factor-1 (NR5A1), in the intestine it is functionally replaced by its close homolog LRH-1 (Liver Receptor Homolog-1, NR5A2) [16-18]. Intestine-specific deletion of LRH-1 abrogates immunological stress-driven intestinal glucocorticoid synthesis and sensitizes for experimentally induced colitis [19, 18]. Similarly, deletion of LRH-1 results in exacerbated immune responses against intestinal viral infections [15, 20]. Of interest, LRH-1 not only regulates intestinal glucocorticoid synthesis, but is also critically involved in intestinal epithelial homeostasis and renewal [21]. LRH-1 is expressed predominantly in the intestinal crypts where it regulates the transcription of cyclin E1 and D1, and thereby the proliferation of stem and early progenitor cells [22]. Given its importance in the regulation of cell cycle, LRH-1 has been proposed as an oncogene. Indeed, LRH-1 is frequently overexpressed in colorectal tumors [23, 24], and genetic deletion of LRH-1 results in reduced development of tumors in murine models of colorectal cancer [25].

Recently, we have shown that human colorectal tumors have maintained the capability to produce immunoregulatory glucocorticoids in an LRH-1-dependent manner [24]. This suggests that LRH-1 may have a dual role in the development of colorectal cancer. On one hand, it may support tumor proliferation via the transcriptional control of cell cycle-regulating genes, on the other hand, it may promote immune evasion by suppressing anti-tumor immune responses via the synthesis of immunoregulatory glucocorticoids [26]. However,

experimental evidence for the latter hypothesis has been lacking to date. Here, we demonstrate that LRH-1 and its inhibitor SHP (Small Heterodimer Partner, NR0B2) are critically involved in the development of inflammation-driven intestinal tumors, by regulating the initial inflammatory phase, which promotes tumor development, as well as the immune escape of established tumors. Employing mice incapable of producing intestinal glucocorticoids, and 3D tumor organoid transplantation, we demonstrate that suppressing anti-tumor immune responses by tumor-derived glucocorticoids is critical for successful tumor growth and development. Finally, gene expression analysis in tumors from human colorectal patients reveals that the expression of genes controlling glucocorticoid synthesis significantly correlates with the expression of immunoregulatory gene products, and overall patient survival. Thus, tumor-derived glucocorticoids may represent a novel immune check point and attractive therapeutic target in the treatment of colorectal tumors.

## Materials and Methods

### Cell lines

The cell line HEK293T had been originally obtained from Inder Verma (Salk Institute). The authentication of the cell line was tested by PCR confirming the presence of the SV40 large T antigen. The murine intestinal epithelial cell line mICcl2 was obtained from Jean-Pierre Kraehenbuehl (Lausanne). The authentication of the cell line was confirmed by flow cytometry confirming E-cadherin expression. All experiments were conducted with mycoplasm-free cell lines.

### Animal studies

All animal experiments were approved by local ethics committee (Regierungspräsidium Freiburg, animal license number G15-88, G17-163) and conducted according to ARRIVE standards. Age- and sex-matched 7 to 11 weeks old mice were used for the experiments. Mice were housed in the at the animal facility of the University of Konstanz under specific pathogen-free conditions with standard diet and water *ad libitum*. All mice were bred under the C57BL/6 genetic background. SHP-deficient mice ($SHP^{-/-}$) [27] and RAG1-deficient mice ($Rag1^{-/-}$) [28] had been described previously. Intestinal epithelial cell-specific LRH-1 knockout mice (villin-Cre x LRH-1 $^{fl/fl}$, LRH-1 $^{IEC\ KO}$) were generated by crossing LRH-1 $^{fl/fl}$ mice with villin-Cre transgenic mice [16]. The littermates lacking the Cre expression (LRH-1 $^{fl/fl}$) were used as controls. LRH-1 $^{IEC\ KO}$ and SHP-deficient mouse lines mice were kindly provided by Kristina Schoonjans (EPFL Lausanne, Switzerland). For all experiments, sibling littermates

were used as controls, with the exception of SHP$^{-/-}$ mice, for which wild type C57Bl/6 mice, housed in the same room, were used.

### Generation of intestine-specific Cyp11b1 knockout mice

The floxed Cyp11b1 mouse line was generated in the Institute Clinique de la Souris in Illkirch, France by targeting exons 3 to 5 of the *Cyp11b1* gene with loxP sites [29]. The resulting Cyp11b1 $^{fl/fl}$ mouse line was crossed with villin-Cre transgenic mice to generate the intestine-specific Cyp11b1-deficient mouse line (Cyp11b1 $^{IEC\ KO}$). The expression of Cre and the successful deletion of floxed exons 3-5 in the small and large intestine was confirmed by PCR (Suppl. Figure 1) using the primers listed in Suppl. Table 1.

### Differential isolation of intestinal epithelial cells along the villus-crypt axis

Intestinal epithelial cells from the small intestine of wild type mice were differentially isolated in 7 fractions from villus to crypts as described previously [15], and used for quantification of LRH-1 target genes by quantitative RT-PCR. For the comparison between wild type and *Shp*$^{-/-}$ mice 4 fractions from villus to crypts were isolated.

### AOM/DSS inflammation-driven colon carcinogenesis model

The AOM/DSS colon carcinogenesis model was performed as described previously [30]. Briefly, female mice were injected i.p. with 12 mg/kg body weight azoxymethane (AOM) (Sigma Aldrich). Five days later, 2.2% (w/v) dextran sulfate sodium (DSS) (molecular weight 36-50 kDa; MP Biomedicals) was given via the drinking water for 5 consecutive days, followed by 16 days normal drinking water. This DSS cycle was repeated 2, resp. 3 times. Body weights were monitored. At time points indicated mice were sacrificed, and colons were removed for macroscopic examination of tumor numbers and size, measurement of colon length, total RNA isolation, and histological or immunohistochemical analysis. Tumor diameter was measured with a sliding caliper and the volume was calculated using the following formula: $V = 4/3\ \pi r^3$. (v: volume, π constant = 3.14 and r: radius = diameter/2).

### Induction of acute colitis

Female wild type and SHP$^{-/-}$ mice were treated with 2.2% (w/v) DSS in the drinking water for 5 days followed by normal drinking water. Control mice received normal drinking water. Body weights were recorded. Mice were sacrificed at day 5, 7 and 10 after DSS treatment. Colons

were longitudinally divided for RNA extraction, histological analysis ("Swiss rolls") and *ex vivo* culture for measurement of colonic glucocorticoid synthesis [16].

### Histopathological and immunohistochemical analyses of colonic tissues

Colonic mouse tissues were fixed in 10% formalin and embedded in paraffin. Paraffin-embedded "Swiss roll" sections were stained with H&E for histopathological evaluation and scored microscopically for colitis using a scoring method described previously [31], ranging from 0 to maximal score of 40.

### Detection of colonic glucocorticoid synthesis

Analysis of colonic glucocorticoid synthesis was done as described previously [15, 18, 32] using a radioimmunoassay. Glucocorticoid synthesis was normalized to tissue weight.

### Colorectal tumor organoids culture

Tumor organoids from wild type, SHP $^{-/-}$, LRH-1 $^{fl/fl}$, LRH-1 $^{IEC\ KO}$, Cyp11b1 $^{fl/fl}$ and Cyp11b1 $^{IEC\ KO}$ mice were generated as described previously [33, 34] with minor modification. In brief, tumors were isolated from AOM/DSS-treated mice at day 56, and digested in digestion buffer. Single cells were washed, seeded into 24-well plates at a density of 15'000 cells per 50 µl Basement Membrane Matrix (BME, Trevigen) per well and overlaid with 500 µl tumor organoid medium [35]. Culture medium was changed every 2 days. Glucocorticoid synthesis was analyzed as described above.

For the analysis of tumor organoid growth, equal numbers of cells were seeded into a 96-well plate in a drop of 8 µl BME diluted 3:4 with medium. Tumor organoids were grown for 4 days, subsequently stained with Hoechst 33342, and the DNA content was analyzed on a plate reader Infinite® 200 PRO (TECAN) as well as by fluorescent microscopy (AXIO Observer.Z1 Microscope, Zeiss) [33].

### Lentiviral transduction of tumor organoids

Production of lentiviral vectors was performed as described [36]. In brief, Cre-lentivirus was produced in HEK293T cells using Cre-IRES-PuroR plasmid (gift from Darrell Kotton, Addgene plasmid #30205) [37] with PAX2 and VSV-G packaging plasmids. Supernatant was passed through a 0.45 µm filter and concentrated (20'000 x g, 1 h, 4 °C). Virus particles were resuspended in Advanced DMEM/F12 supplemented with 10 mM HEPES, 1x Glutamax, 1x

penicillin/streptomycin and stored at -80° C. Lentiviral transduction of organoids was performed as described [36]. Briefly, organoid cells were singularized by pipetting several times and subsequent Accutase digestion. After washing, cells were spinfected (500 x g, 1 h, 32° C) with 8 µg/ml polybrene. After incubation for 3 h, cells were seeded in BME and selection was started after 48 h with 1 µg/µl puromycin.

**Subcutaneous transplantation of tumor organoids**

Subcutaneous transplantation of tumor organoids was performed as described previously [38] with minor modification. Organoids were dissociated into small cell clusters. Two x $10^5$ cells were resuspended in organoid basal medium, mixed with 50% BME to a final volume of 200 µl, and injected subcutaneously into the flanks of C57BL/6 wild type mice. In some experiments, also lymphopenic Rag1$^{-/-}$ recipient mice were used. Tumor sizes were measured using sliding caliper and tumor volume was calculated as 0.523 × length × width × width. At day 12 or 24 after subcutaneous transplantation, mice were euthanized, subcutaneous tumors were collected, individual tumor weight and volume were measured, and tumors were used for histological and flow cytometry analysis. In some experiments wild type recipient mice were treated with 0.28 mg/ml dexamethasone in the drinking water ad libitum as described previously [39].

**Flow Cytometry**

Tumors were isolated 9 or 12 days after s.c. transplantation of tumor organoids, and digested in DMEM medium containing 10% FCS, 0.75 mg/ml collagenase IV (Sigma-Aldrich, St. Louis, MO), 40 µg/ml DNase I (Roche Diagnostics, Indianapolis, IN) and 3 mM $CaCl_2$. Digestion was stopped using 30 µl 0.5 M EDTA and cells were filtered through a 40 µm cell strainer to obtain single cell suspension. Dead cell staining was performed before blocking and staining steps using the Fixable Viability Dye eFluor 455UV (65-0868-14, eBioscience, San Diego, CA). Cells were blocked afterwards with 3% bovine serum albumin (BSA) and anti-CD16/32 TruStain FcX™ PLUS antibody (156603, BioLegend, San Diego, CA), and stained using following surface marker detecting, fluorochrome-conjugated antibodies purchased from BioLegend (San Diego, CA): anti-Ly-6G-BV605 (127639), anti-NK-1.1-BV711 (108745), anti-Ly-6C-BV785 (128041), anti-CD26-FITC (137805), anti-XRC1-PE (148204), anti-CD64-AF-647 (139321), anti-CD45-AF-700 (103128), anti-CD11b-PE-Cy7 (101216), from eBioscience (San Diego, CA): anti-CD11c-PE-eFluor 610 (61-0114-80), anti-MHCII-APC-eFluor 780 (47-5321-80), anti-CD3-eFluor 506 (69-0032-80), anti-CD19-eFluor 506 (69-0193-80) and anti-Siglec-F-BV421 (565934, BD Biosciences, Franklin Lakes, NJ). Flow Cytometry experiments were performed with LSRFortessa (BD Biosciences, Franklin

Lakes, NJ) and data were pre-processed using FlowJo software (BD Life Sciences, Ashland, Oregon).

### High dimensional FlowSOM algorithm-guided analysis

High dimensional flow cytometry analysis of tumor-infiltrating immune cells was performed according to the workflow as previously described [40, 29]. Compensation-corrected FCS files were cleaned, preprocessed and single, live cells were manually gated after sequential doublet discrimination and exported using FlowJo software (BD Life Sciences, Ashland, Oregon). Exported FCS files were uploaded into RStudio environment and data transformation was performed by applying the inverse hyperbolic arcsinh function with individually set cofactors. Data were further transformed with the *matrixStats* R package to normalize all marker expression between values of 0 and 1 with low (1%) and high (99%) percentiles as a limit. Each FCS sample was downsampled to 10'000 cells and combined for the Uniform Manifold Approximation and Projection (UMAP) projection using the *umap* R package [41]. FlowSOM algorithm-based clustering with 100 self-organizing map codes (by default) was applied on the combined data set and metaclustering was performed using the *ConsensusClusterPlus* package with $k$=27 [42]. Cluster distribution was visualized with UMAP. FlowSOM clusters were manually merged and annotated to 18 identified cell populations based on their lineage marker expression profiles.

### RNA isolation and quantitative RT-PCR

Total RNA from murine tissues and tumors was isolated using peqGOLD TriFast™ (Peqlab) or RNA isolation kits (Promega) according to manufacturer's instructions, and RNA was reverse transcribed. cDNA was analyzed for gene expression by real time PCR using SYBR® Green PCR Master Mix on a One-Step-Plus realtime PCR machine (Applied Biosystems) and normalized to β-actin. Primers used are listed in suppl. Table 1.

### LRH-1 reporter activity

The murine intestinal epithelial cell line mICcl2 was transfected with LRH-1 expression vector, an LRH-1 luciferase reporter (mLRH-1 5xRE) and increasing concentrations of SHP expression vector [17]. LRH-1 transcriptional activity was measured in a luciferase reporter assay. In other experiments, mICcl2 cells were transfected with LRH-1 and increasing concentrations of SHP expression vector, and luciferase reporter construct for the promoter of LRH-1 target genes *Cyp11a1* and *Cyp11b1* [17].

**Co-precipitation experiment**

HEK293T cells were co-transfected with Myc/His-tagged β-galactosidase or Myc/His-tagged SHP, and GFP-tagged LRH-1 expression plasmid using the calcium phosphate method. Cells were then lysed in buffer A (10 mM Hepes, 10 mM KCl, pH 7.9, 1 mM DTT, universal protease inhibitor (Roche), 1% NP-40) for 10 min at RT. Nuclei were pelleted at 20'000 x g for 4 min at 4°C, and lysed in buffer B (20 mM Hepes, 500 mM NaCl, 10% glycerol, 1 mM DTT, protease inhibitor) at 4°C for 30 min. After centrifugation at 1'700 x g nucleoplasm was isolated, and incubated with $Ni^{2+}$-sepharose-beads (NiNTA, Sigma*)* for 30 min at RT. Subsequently, beads were washed 10 times in PBS, 1% Tween, 10 mM Imidazol, pH 8.0. Protein complexes were eluted in 1x PBS, 500 mM Imidazol, pH 8.0 and analyzed by Western blotting using anti-Myc-tag and GFP-tag antibodies.

**Analysis of human gene expression data**

Clinical data as well as gene expression (FPKM - Fragments Per Kilobase of transcript per Million) for target genes (TG) of 379 Colon Adenocarcinoma (COAD) patients with any stage (I-III excluding stage IV and patients indicated as clinical stage Not Available (NA)) of disease were downloaded from TCGA Data portal (https://portal.gdc.cancer.gov/files/4060482f-eedf-4959-97f1-f8b6c529c368, Release Date: 2018-08-23; Release Number 12.0). We next stratified the patients in two groups according to their TG expression (group top containing patients with high expression - as the upper quartile and, the group low containing patients with lower expression - lower quartile for each of the TG: CYP11A1, HSD11B1, HSD11B2, NR0B2, or NR5A2). The Kaplan-Meier estimator provided in the R language package was used for comparing the overall survival distributions between the high vs. low groups. The TCGA data and R script used to perform the Kaplan-Meier analysis are available within the Supplementary Information. Lastly, the comparison of immune gene expression between the high vs. low groups was performed using the nonparametric Wilcoxon's signed rank test. Gene expression levels were expressed as the log RPKM - Reads per kilobase per million mapped reads.

**Statistical data analysis**

The statistical analysis of mouse experiments was performed using Graphpad Prism software (version 6). Statistical tests used were unpaired student's T-test when comparing two groups and two-way ANOVA followed by Tukey's multiple comparison test when

comparing multiple groups. The Kaplan-Meier method was used to estimate survival distribution between the groups and log-rank tests were applied to compare survival rates.

For the analysis of human gene expression data, the Kaplan-Meier estimator provided in the R-language package was used for comparing the overall survival distributions between the high *versus* low groups. Lastly, the comparison of immune gene expression between the high *versus* low groups was performed using the non-parametric Wilcoxon's signed rank test.

A p value $< 0.05$ was set as the level of significance.

## Results

### LRH-1 regulates inflammation-driven intestinal tumor development

We and others have previously shown that LRH-1 regulates both intestinal steroidogenesis [16, 18] as well as intestinal tumor development [25], yet, the direct association of both processes has not been assessed so far. We thus set out to investigate the impact of intestinal epithelium-specific deletion of LRH-1 in a murine model of inflammation-driven colorectal tumor development. A single injection of the mutagen azoxymethane (AOM), followed by 3 cycles of dextran sodium sulfate (DSS)-driven intestinal inflammation (Figure 1A) results in the robust development of colonic adenomas [43]. Treatment of mice with DSS caused an inflammation-driven weight loss, which was restored when mice were exposed to normal drinking water [32]. In line with our previous observation that LRH-1 regulates intestinal immune homeostasis and inflammation [25] via the synthesis of immunoregulatory glucocorticoids [19, 16, 18], we observed a substantial increase in weight loss of mice with intestine-specific (villin-Cre-mediated) deletion of *Lrh-1* (LRH-1 $^{IEC\ KO}$), suggesting increased intestinal inflammation after DSS treatment (Figure 1B). We next assessed the tumor development after 3 cycles of DSS. As expected at day 56 post AOM treatment we observed smaller intestinal tumors in mice, which lacked intestinal *Lrh-1* expression (Figure 1C, D). While the absolute number of detectable tumors was not significantly different, LRH-1 deficiency clearly resulted in much smaller tumors than in wild type mice (Figure 1E, F). Thus, these data confirm the crucial role of LRH-1 in regulating intestinal inflammation and tumor development [19, 16, 25].

### SHP regulates LRH-1 activity

These experiments, however, also revealed that while inflammation is essential for driving tumor development in this mouse model, LRH-1-regulated processes appear to be more

critical in regulating tumor growth, as LRH-1 $^{IEC\ KO}$ mice showed more severe chronic colitis (Figure 1B), yet developed smaller tumors (Figure 1E). To analyze the tumor-promoting role of LRH-1 in more detail, we set out to experimentally enhance LRH-1 activity. SHP (Small Heterodimer Partner, NR0B2) is one of the important transcriptional targets of LRH-1. At the same time, SHP binds and inhibits LRH-1, and thus restricts LRH-1 activity in a negative feedback loop [44, 45, 17, 46]. In pulldown experiments we confirmed the direct physical interaction between LRH-1 and SHP (Figure 2A). Furthermore, SHP overexpression dose-dependently inhibited LRH-1 transcriptional activity (Figure 2B-D). Importantly, in the small intestine, large intestine and the differentially isolated epithelial cells along the crypt-villus axis of wild type mice, SHP was found to be co-expressed with LRH-1 and the LRH-1 target genes, the steroidogenic enzymes *Cyp11a1* and *Cyp11b1*, and *Ccne1* (cyclin E1), in the intestinal tissue and the intestinal crypts (Figure 2E and F). Thus, intestinal SHP expression may regulate LRH-1 activity in the intestinal epithelium.

**SHP-deficient mice develop less inflammation-driven intestinal tumors**

We next assessed whether genetic deletion of SHP would unleash the oncogenic activity of LRH-1 resulting in increased AOM/DSS-induced intestinal tumors. We first confirmed that SHP expression was undetectable in the intestine of SHP (*Nr0b2*)-deficient mice (Figure 3A), and that SHP-deficiency resulted in increased LRH-1 transcriptional activity. While *Lrh-1* (*Nr5a2*) expression was only slightly increased (Figure 3B), the expression of the LRH-1 target gene cyclin D1 (*Ccnd1*) [22] was up to 3 times higher in the crypts of SHP-deficient mice (Figure 3C), supporting the idea that increased LRH-1 activity results in increased target gene expression. When SHP-deficient mice were exposed to AOM and 3 cycles of DSS, reduced inflammation-driven weigh loss was recorded (Figure 3D), indicating that SHP deficiency was able to unleash the anti-inflammatory activity of LRH-1. Surprisingly, however, when tumor development and growth was assessed at days 56 and 64 post AOM/DSS treatment, a significantly reduced number and size of colorectal tumors was noticed in SHP-deficient animals (Figure 3E-H). Reduced tumor growth correlated also with an increased survival of SHP-deficient mice compared to wild type mice (Figure 3I).

**SHP deficiency ameliorates acute DSS-induced colitis**

Since AOM/DSS-induced tumor development strongly depends on the chronic intestinal inflammation, we investigated whether reduced inflammation in SHP-deficient mice could be responsible for the reduced development of intestinal tumors. Indeed, when SHP-deficient mice were exposed to acute DSS-induced colitis (Figure 4A), a significant delay in weight loss was noticed (Figure 4B). This was accompanied by reduced inflammation-driven colon

shortening (Figure 4C) and colitis score (Figure 4D). In line with the increased activity of LRH-1 in SHP-deficient mice, we observed increased colitis-induced expression of the steroidogenic enzymes *Cyp11a1* and *Cyp11b1* (Figure 4E, F), and associated production of colonic corticosterone (Figure 4G). In parallel, a significant increase of the immunosuppressive cytokine interleukin (IL)-10 and a trend towards reduced tumor necrosis factor (TNF) expression was noticed in SHP-deficient mice at the peak of DSS colitis at day 7, while LRH-1 expression was not different (Figure 4H-J). Thus, SHP deficiency is associated with reduced DSS-induced inflammation, and increased immunoregulatory corticosterone synthesis and IL-10 expression.

**Intestinal glucocorticoid synthesis regulates tumor development and growth**

We next aimed at more specifically investigating the relative contribution of intestinal steroidogenesis in the development of inflammation-driven intestinal tumor development. For this purpose, we developed a novel mouse model with defective intestinal glucocorticoid synthesis. 11β-hydroxylase, encoded by the gene *Cyp11b1*, converts the inactive precursor molecule deoxycorticosterone to the active glucocorticoid corticosterone. We thus generated a mouse line, where exons 3-5 of the *Cyp11b1* gene were deleted in the intestinal epithelium using villin promoter-driven Cre recombinase expression (Cyp11b1 $^{IEC\ KO}$) (Suppl. Figure 1A-C). As expected, the intestinal epithelium of these conditional knockout mice showed a drastically reduced expression of *Cyp11b1* (Suppl. Figure 1D) and immune cell-driven corticosterone production (Suppl. Figure 1F, G), while the adrenal synthesis of glucocorticoids remained unaffected (Suppl. Figure 1E). These data confirm the intestine-specific deletion of *Cyp11b1* and associated loss of intestinal glucocorticoid synthesis.

We next induced intestinal tumor development in these mice by AOM injection and chronic DSS colitis (Figure 5A). Interestingly, while Cyp11b1 $^{IEC\ KO}$ mice showed significantly increase body weight loss in the first two cycles of DSS, suggesting increased intestinal inflammation in the absence of immunoregulatory glucocorticoids, Cyp11b1 $^{IEC\ KO}$ mice recovered faster after the third cycle of DSS (Figure 5B). In line with increased inflammation, we also observed an increase in colonic tumors in Cyp11b1 $^{IEC\ KO}$ mice at day 35 after 2 cycles of DSS, but a significant reduction in tumor numbers at day 56 (Figure 5C, D). Cyp11b1-deficient mice not only showed reduced tumor numbers, but tumors were also smaller. Furthermore, Cyp11b1-deficient tumors had reduced expression of the immunoregulatory molecules CD274 (PD-L1), CD152 (CTLA-4) and IL-10 (Figure 5E). This observation likely reflects the immunosuppressive effects of glucocorticoids released from already established tumors, enabling immune escape.

**Transplantation of 3D tumoroids reveals the oncogenic potential of LRH-1**

These experiments described above demonstrated that LRH-1 and intestinal glucocorticoid synthesis may affect inflammation-driven intestinal tumorigenesis at two different levels. While LRH-1 is critical for tumor growth via the transcriptional regulation of cell cycle-regulating genes, it also controls inflammation via the regulation of glucocorticoid synthesis in the normal intestinal epithelium, and thereby limits colitis-induced tumor development. On the other hand, tumor-expressed LRH-1 and associated glucocorticoid synthesis by intestinal tumors may favor immune escape and thus promote tumor development and growth. To analyze these processes independently of the initial tumor-promoting inflammatory phase during the chronic colitis, we isolated tumors from wild type mice, LRH-1-deficient or SHP-deficient mice at day 56, and expanded tumor cells in 3D-cultures resulting in tumor organoids (tumoroids) (Figure 6A, Suppl. Figure 2A). Although LRH-1 regulates cell growth, wild type, LRH-1-deficient as well as SHP-deficient tumoroids could be expanded *in vitro* (Suppl. Figure 2B-E). When tumoroids were sufficiently expanded, they were transplanted s.c. into wild type immunocompetent C57Bl/6 mice. Importantly, each recipient mouse was simultaneously transplanted with wild type tumoroids and LRH-1-, resp. SHP-deficient tumoroids, to directly compare tumor growth. Tumoroids grew very rapidly to a palpable size at day 6-12 post transplantation. In line with the oncogenic role of LRH-1 a significantly reduced growth was observed for LRH-1-deficient tumoroids (Figure 6B-E). Interestingly, while in transplanted wild type tumoroids tumor cells were interspersed in tumor stroma, almost no LRH-1-deficient tumor cells were detectable anymore at day 12. In contrast, increased immune cell infiltrates were evident (Figure 6F). As expected, the opposite phenotype was observed when SHP-deficient tumoroids were transplanted. In line with unleashed LRH-1 activity, they grew significantly faster and bigger than wild type tumoroids (Figure 6G-K).

**Tumor-derived glucocorticoids favor tumor growth and immune escape**

We next aimed to address the relative contribution of LRH-1-regulated tumor-autonomous glucocorticoid synthesis in the expansion of transplanted tumors. We thus first confirmed that wild type tumoroids produce glucocorticoids, whereas Cyp11b1-deficient tumoroids produce less (Suppl. Figure 2F). Strikingly, while control tumoroids expanded rapidly after transplantation, a significant delay was monitored in Cyp11b1 $^{IEC\ KO}$ tumoroid transplants (Figure 7A, D). This was also reflected by the weight of the tumors at day 12 post transplantation (Figure 7C). Importantly, no difference in control or Cyp11b1 $^{IEC\ KO}$ tumoroid growth was observed *in vitro* (Suppl. Figure 2C). These data support the notion that tumors incapable of releasing immunoregulatory glucocorticoids are controlled more efficiently by

the immune system. To provide further evidence for the hypothesis that glucocorticoids mediate tumor immune evasion, wild type recipient mice were control treated or received the synthetic glucocorticoid dexamethasone in the drinking water. Notably, while in untreated recipient mice Cyp11b1-proficient tumors grew faster and bigger than Cyp11b1-deficient ones, no statistical difference was observed anymore in dexamethasone-treated recipient mice (Suppl. Figure 3A). Similarly, when Cyp11b1 was deleted *in vitro* by transducing Cyp11b1L/L tumor organoids with lentiviral Cre recombinase, a similar growth advantage of Cyp11b1-proficient tumors over Cyp11b1-deleted tumors was observed upon s.c. transplantation (Suppl. Figure 3B-E). These findings support the idea that lack of tumor glucocorticoid synthesis, rather than differences in genetic mutations, is responsible for the reduced growth observed. We next transplanted Cyp11b1-proficient and Cyp11b1-deficient tumoroids into lymphopenic Rag1-deficient mice to monitor the contribution of T and B cells in the control of tumor growth. Interestingly, while we could still see enhanced growth of control tumoroids, differences to Cyp11b1-deficient tumoroids were less pronounced than when transplanted into wild type recipients (Figure 7B). Importantly, when tumor sizes were analyzed at day 12 post transplantation no significant difference was observed (Figure 7E, F). These findings suggest a contribution of immune cells, in part also lymphocytes, in the control of tumor growth, which is suppressed by tumor-derived glucocorticoids.

In support of this notion, we detected reduced expression of the M2-like macrophage marker arginase 1 (*Arg1*), but increased expression of the pro-inflammatory cytokine IL-6 in Cyp11b1-deficient transplanted tumoroids. While IL-10 expression was not significantly different, there was a tendency towards lower expression in Cyp11b1-deficient tumors ($p = 0.0837$) (Suppl. Figure 4A). These changes were paralleled by a significant increase in $CD45^+$ and $CD11b^+$ leukocytes, while levels of $CD3^+$ and $FoxP3^+$ regulatory T cells were not significantly different (Suppl. Figure 4B). To further characterize the differences in tumor-infiltrating immune cells, we employed high dimensional flow cytometry with computational clustering and analysis of immune cell populations (Suppl. Figure 4C, Figure 7G-I). These analyses of immune cell infiltrates in Cyp11b1-proficient and Cyp11b1-deficient transplanted tumors revealed substantial changes in innate immune cell populations, especially dendritic cells, macrophages, NK cells and neutrophils at day 9 post transplantation (Figure 7I).

## Survival of colorectal tumor patients negatively correlates with the expression of steroidogenic factors and immunomodulatory markers

In order to assess the potential relevance of our findings for the pathogenesis of human colorectal cancer, we analyzed the expression profile of *CYP11A1*, *HSD11B1*, *HSD11B2*, *NR5A2* (LRH-1) and *NR0B2* (SHP) in tumors from 379 colorectal cancer patients, and

correlated their overall survival to the expression of these steroidogenic factors. CYP11A1 (p450 side chain-cleaving enzyme) is the rate-limiting and thus essential enzyme in the *de novo* synthesis of glucocorticoids from cholesterol, whereas HSD11B2 (hydroxysteroid dehydrogenase 11B2) deactivates cortisol to cortisone, and HSD11B1 reactivates cortisone to cortisol and thus contributes to the regulation of local glucocorticoid levels (reviewed in [26, 13]). When patients were stratified into high expressors (highest quartile) and low expressors (lowest quartile), a significant difference in patient overall survival could be seen for *CYP11A1*, *HSD11B1* and *NR0B2* (Figure 8A), but not for *NR5A2* and *HSD11B2* (Suppl. Figure 5A). Interestingly, while high *CYP11A1* and *HSD11B1* expression resulted in poor survival, suggesting that tumors efficiently suppressing the immune system via glucocorticoids have a growth advantage, high *NR0B2* was beneficial for survival, likely due to increased suppression of LRH-1. The proposed role of tumor glucocorticoid synthesis in suppressing anti-tumor immune responses was further supported by the observation that high *CYP11A1* and *HSD11B1* expression also resulted in a significantly increased expression of the immunosuppressive cytokines TGFβ1 and IL-10, the immune checkpoint molecules CD279 (PD-1), CD274 (PD-L1) and CD152 (CTLA-4), and the M2-like macrophage markers LAYN, CCR4 and ARG1 [47]. In contrast, high *NR0B2* expression correlated with a significantly lower expression of these immune markers (Figure 8B). These findings support the hypothesis that glucocorticoid synthesis in colorectal tumors results in a suppressive tumor microenvironment, favoring the escape of the tumor from destruction by the immune system and worse patient survival.

## Discussion

It is currently well accepted that the immune system critically regulates tumor development. A limiting aspect in tumor immune surveillance, however, are all the factors that control self-tolerance, and thus limit the activation of tumor-specific immune cells. Currently best studied are the immune checkpoint molecules PD-1/PD-L1 and CLTA-4. The recognition of the importance of these immune checkpoints for controlling the immune system in general, and anti-tumor responses in particular, has led to the development of neutralizing antibodies against these checkpoint molecules and their successful use as therapeutic agents. The results in the treatment of some, but not all tumors are astonishing, in particular in combination with conventional chemotherapy. Yet, the unsuccessful treatment of many patients clearly indicates that other potential immune checkpoints may exist.

Here we provide evidence that tumor–derived glucocorticoids may indeed represent such a novel “checkpoint”, and that inhibition of tumor glucocorticoid synthesis could develop as an effective therapeutic approach. Although we transplanted syngeneic tumors into syngeneic recipient mice, in the absence of dominant tumor model antigens, our data point out that inhibition of glucocorticoid synthesis in tumors alone is sufficient to promote a protective immune response, causing a strong reduction in tumor growth. Importantly, differences in genetic mutations of the transplanted tumors could be excluded as *in vitro* deletion of the *Cyp11b1* gene in tumor organoids by lentiviral Cre transduction resulted in similar reduced tumor growth upon s.c. transplantation. To which extent this immune surveillance is mediated by tumor-specific T lymphocytes, innate immune cells, such as natural killer cells and neutrophils, or a combination thereof [48-50], remains to be determined. Clearly, Cyp11b1-deficient tumors still grew slower, even in T cell-depleted Rag-deficient mice (Figure 7B), and had increased numbers of infiltrating macrophages, dendritic cells, neutrophils and NK cells (Figure 7I). Thus, is very likely that both, cells of the adaptive and innate immune system contribute to the control of tumor growth. Furthermore, the relative contribution of cells of the innate and adaptive immune system may be different during the development of primary, inflammation-driven intestinal tumors *versus* the transplantation of tumor organoids.

Excitingly, our experimental data in mice also strongly correlated with the gene expression and survival data in human colorectal cancer patients. The expression levels of the two steroidogenic enzymes CYP11A1, promoting *de novo* synthesis of glucocorticoids from cholesterol, and HSD11B1, initiating reactivation of glucocorticoids from inactive precursors (reviewed in [12, 13]), significantly correlated with the overall patients’ survival (Figure 8A). In marked contrast, high expression of SHP, likely by suppressing LRH-1 and associated proliferation and steroidogenesis, positively correlated with patient survival. These data indeed suggest that glucocorticoid synthesis in colorectal tumor patients actively suppresses tumor surveillance by the immune system. In support of this idea is also our observation that high expression of the steroidogenic enzymes CYP11A1 and HSD11B1 correlated with high expression of the immunosuppressive cytokines TGFβ and IL-10, the immune checkpoint molecules PD-1, PD-L1 and CTLA-4, and the presence of $LAYN^+$ and $CCR4^+$ tumor-associated M2-like macrophages (Figure 8B). A similar pattern of immune markers was also observed in primary mouse tumors (Figure 5E). In support of this idea, it was recently observed that glucocorticoids upregulate immune checkpoint molecules in the tumor microenvironment [51, 52]. Thus, tumor-autonomous glucocorticoid synthesis appears to substantially condition the tumor microenvironment, ultimately suppressing anti-tumor immune responses and resulting in decreased patient survival. Somewhat surprising was the observation that expression levels of LRH-1 did not significantly affect patients’ survival.

While the underlying reason is difficult to reconcile, it has to be considered that LRH-1 is involved in the transcriptional control of a broad spectrum of processes, including proliferation, survival, metabolism and steroidogenesis, which may have even conflicting effects on tumor development. In contrast, expression levels of steroidogenic enzymes represent only one spectrum of LRH-1 target genes and will thus affect only the steroidogenic capacity of colorectal tumors.

A major aim of this study has been to investigate the relative contribution of LRH-1-regulated glucocorticoid synthesis in the inflammation-induced development of colorectal tumors. Our results point out that intestinal glucocorticoid synthesis has a prominent dual role in this process. At the early phase, LRH-1-regulated intestinal glucocorticoid synthesis appears to suppress intestinal inflammation and thus associated tumor development. Along these lines, we have seen that intestine-specific deletion of *Cyp11b1*, abrogating intestinal glucocorticoid synthesis, resulted in increased inflammation and increased tumor development during the early phases of chronic colitis (Figure 5B-D). In contrast, deletion of SHP resulted in increased LRH-1-regulated steroidogenesis and reduced inflammation-driven tumor development. Thus, deletion of SHP was able to unleash the anti-inflammatory activity of LRH-1, rather than its oncogenic potential. Of interest is the observation that although deletion of LRH-1 resulted in increased inflammation, rather reduced tumor development was observed. This illustrates that increased inflammation *per se* is insufficient to promote tumor development, but that the proliferation-promoting activity and likely also the glucocorticoid-promoting activity of LRH-1 in already established tumors is necessary for efficient tumor growth and survival. In support of this hypothesis, we have seen that in the absence of an inflammatory environment (i.e. in the transplantation experiment) deletion of SHP was able to promote the oncogenic activity of LRH-1, resulting in increased growth of transplanted tumoroids (Figure 6G-K). While these experiments do not reveal the relative importance of LRH-1 in regulating tumor growth via the transcriptional control of cell cycle-regulating genes *versus* the suppression of anti-tumor immune responses via tumor-derived glucocorticoids, the transplantation of Cyp11b1-deficient tumoroids, which maintain-LRH-1-regulated proliferation, clearly support the idea that the local synthesis of glucocorticoids critically contributes to the evasion of colorectal tumors from tumor immune surveillance, and thus promotes their survival and growth. In line with this concept is our observation that although Cyp11b1-deficient mice showed increased tumor development during the early phase of chronic colitis (day 35) due to increase inflammation-driven tumor development, the opposite was seen after the third cycle of DSS (day 56) (Figure 5C, D), indicating that in already established tumors glucocorticoid-mediated immune evasion is essential for their survival. Furthermore, we have seen that treatment of recipient mice with dexamethasone abolished

the growth differences between Cyp11b1-proficient and deficient tumoroids after transplantation (Suppl. Figure 3).

While the oncogenic role of LRH-1 has been well documented in a variety of tumors, the role of steroidogenic enzymes in the development of tumors, and colorectal tumors in particular, is less clear. In colon cancer *CYP11A1* appears to be frequently downregulated [53]. Nonetheless, our own data demonstrate that high *CYP11A1* expression results in increased tumor growth and reduced patient survival. Interestingly, certain *CYP11A1* polymorphisms have also been associated with an increased risk to develop breast cancer. In addition, *CYP11B1*, encoding 11β-hydroxylase, has been reported to be frequently mutated in different tumors, including colorectal tumors [53]. Although the impact of these mutations on the expression and function of this enzyme has not been studied so far, it is very likely that they are part of a selection process during tumor development. Of interest, while we have seen significant differences in overall patient survival between tumors with high versus low *CYP11A1* expression (Figure 8A), we have not been able to conduct the same analysis for *CYP11B1*, as expression was not reported for all tumor tissues summarized in the TCGA data base. One of the underlying reasons may well be that basal expression levels of *CYP11B1* may be lower than those of *CYP11A1*. This notion is in line with our previous observation in the murine intestine, where *Cyp11b1* was barely detectable in control mice, but strongly upregulated upon immune cell activation or by inflammation (suppl. Figure 1D) [18, 32, 54]. Most importantly, 11β-hydroxylase appears to be essential for glucocorticoid synthesis in the intestinal epithelium and intestinal tumors, as *Cyp11b1* deletion abrogated it (suppl. Figure 1F, G).

Based on the here discussed role of tumor-derived glucocorticoids in immune escape, LRH-1-regulated steroid synthesis in tumor cells may represent an attractive new therapeutic approach. However, a general suppression of glucocorticoid synthesis will likely result in severe side-effects, given the wide-spread roles of glucocorticoids in numerous physiological processes. Thus, a detailed understanding of the tumor-specific processes controlling glucocorticoid synthesis in colorectal cancer may be instrumental to develop tumor-specific therapies. In this regard LRH-1 seems to be a most promising target.

**Conclusions**

We have previously shown that human colorectal tumor cells are capable of producing immunoregulatory glucocorticoids in an LRH-1-regulated manner. In this study, we now

specifically addressed how tumor-derived glucocorticoids regulate anti-tumor immune responses and tumor growth in a murine model of inflammation-driven colorectal tumor development. Our results show that tumors lacking LRH-1 expression or its transcriptional target Cyp11b1 fail to produce tumor-autonomous glucocorticoids, which results in a better control of the tumor growth by tumor-infiltrating immune cells. Thus, tumor-derived glucocorticoids appear to be an important immune checkpoint. Comparative gene expression and survival data analysis indicate that similar immune escape mechanisms exist also in human colorectal cancer patients.

**Acknowledgments**

The authors would like to thank the members of the Brunner lab for their support, Christian Schmidt for graphical support, Kristina Schoonjans for the LRH-1 $^{IEC\ KO}$ and SHP-deficient mouse lines, and Stephen Tait for comments and suggestions. The authors remember gratefully Marcus Groettrup, who passed away way too early.

This work was supported by the German Research Foundation (grants BR3369/4-2, BR3369/9-1) to T.B., by the LOEWE Center "Frankfurt Cancer Institute" funded by the Hessen State Ministry for Higher Education, Research and the Arts (III L 5–519/ 03/ 03.001 - (0015)) and the DFG research group "Cell plasticity in CRC" (FOR2438) to H.F.F., the Brazilian National Council for Scientific and Technological Development (CNPq) to K.J.G., Sao Paulo Research Foundation (FAPESP) to K.J.G. A.A was supported by a Fellowship from the Ministry of Higher Education and Scientific Research, Sudan and a Fellowship from the Baden-Württemberg-Stiftung. K.B. Fellowship from the Baden-Württemberg Ministry of Science, Research and Art–funded Co-operative research training school 'Advanced in-vitro test systems for the analysis of cell-chemical interactions in drug discovery and environmental safety' (InViTe).
Authors declare that they have no competing financial interests.

**Author contributions:** A.A. planed and conducted most experiments, and generated the figures; C.R., E.B., C.U., M.N., T.S.P., L.D., V.M.M., F.K., and F.N. conducted some experiments; F.K. and R.S. characterized the Cyp11b1 $^{IEC\ KO}$ mouse model; J.K. helped with the AOM/DSS tumor model; K.B., C.M. and H.F.F. helped with the tumoroid system; A.P.P. contributed to the figure generation; I.T.S. and K.J.G. analyzed the gene expression data bases; E.K. advised on clinical samples; T.B. supervised the study and wrote the manuscript.

**Conflict of Interest:** All authors declare no conflict of interest.

**Data availability:** The datasets generated during and/or analyzed during the current study are available from the corresponding authors on reasonable request.

## References


1. Burnet FM (1970) The concept of immunological surveillance. Prog Exp Tumor Res 13, 1-27
2. Galon J, Costes A, Sanchez-Cabo F, Kirilovsky A, Mlecnik B, Lagorce-Pages C, Tosolini M, Camus M, Berger A, Wind P, Zinzindohoue F, Bruneval P, Cugnenc PH, Trajanoski Z, Fridman WH & Pages F (2006) Type, density, and location of immune cells within human colorectal tumors predict clinical outcome. Science 313, 1960-1964
3. Pages F, Berger A, Camus M, Sanchez-Cabo F, Costes A, Molidor R, Mlecnik B, Kirilovsky A, Nilsson M, Damotte D, Meatchi T, Bruneval P, Cugnenc PH, Trajanoski Z, Fridman WH & Galon J (2005) Effector memory T cells, early metastasis, and survival in colorectal cancer. N Engl J Med 353, 2654-2666
4. Angell HK, Bruni D, Barrett JC, Herbst R & Galon J (2019) The Immunoscore: Colon Cancer and Beyond. Clin Cancer Res 26, 332-339
5. Saito T, Nishikawa H, Wada H, Nagano Y, Sugiyama D, Atarashi K, Maeda Y, Hamaguchi M, Ohkura N, Sato E, Nagase H, Nishimura J, Yamamoto H, Takiguchi S, Tanoue T, Suda W, Morita H, Hattori M, Honda K, Mori M, Doki Y & Sakaguchi S (2016) Two FOXP3(+)CD4(+) T cell subpopulations distinctly control the prognosis of colorectal cancers. Nat Med 22, 679-684
6. Laviron M & Boissonnas A (2019) Ontogeny of Tumor-Associated Macrophages. Front Immunol 10, 1799
7. Garrido F, Ruiz-Cabello F & Aptsiauri N (2017) Rejection versus escape: the tumor MHC dilemma. Cancer Immunol Immunother 66, 259-271
8. Picon A, Gold LI, Wang J, Cohen A & Friedman E (1998) A subset of metastatic human colon cancers expresses elevated levels of transforming growth factor beta1. Cancer Epidemiol Biomarkers Prev 7, 497-504
9. Hahne M, Rimoldi D, Schroter M, Romero P, Schreier M, French LE, Schneider P, Bornand T, Fontana A, Lienard D, Cerottini J & Tschopp J (1996) Melanoma cell expression of Fas(Apo-1/CD95) ligand: implications for tumor immune escape. Science 274, 1363-1366
10. Niehans GA, Brunner T, Frizelle SP, Liston JC, Salerno CT, Knapp DJ, Green DR & Kratzke RA (1997) Human lung carcinomas express Fas ligand. Cancer Res 57, 1007-1012
11. Galluzzi L, Buque A, Kepp O, Zitvogel L & Kroemer G (2017) Immunogenic cell death in cancer and infectious disease. Nat Rev Immunol 17, 97-111
12. Noti M, Sidler D & Brunner T (2009) Extra-adrenal glucocorticoid synthesis in the intestinal epithelium: more than a drop in the ocean? Semin Immunopathol 31, 237-248
13. Phan TS, Merk VM & Brunner T (2019) Extra-adrenal glucocorticoid synthesis at epithelial barriers. Genes Immun 20, 627-640
14. Taves MD, Gomez-Sanchez CE & Soma KK (2011) Extra-adrenal glucocorticoids and mineralocorticoids: evidence for local synthesis, regulation, and function. American journal of physiology Endocrinology and Metabolism 301, E11-24
15. Cima I, Corazza N, Dick B, Fuhrer A, Herren S, Jakob S, Ayuni E, Mueller C & Brunner T (2004) Intestinal epithelial cells synthesize glucocorticoids and regulate T cell activation. J Exp Med 200, 1635-1646
16. Coste A, Dubuquoy L, Barnouin R, Annicotte JS, Magnier B, Notti M, Corazza N, Antal MC, Metzger D, Desreumaux P, Brunner T, Auwerx J & Schoonjans K (2007) LRH-1-mediated glucocorticoid synthesis in enterocytes protects against inflammatory bowel disease. Proc Natl Acad Sci U S A 104, 13098-13103
17. Mueller M, Atanasov A, Cima I, Corazza N, Schoonjans K & Brunner T (2007) Differential regulation of glucocorticoid synthesis in murine intestinal epithelial versus adrenocortical cell lines. Endocrinology 148, 1445-1453
18. Mueller M, Cima I, Noti M, Fuhrer A, Jakob S, Dubuquoy L, Schoonjans K & Brunner T (2006) The nuclear receptor LRH-1 critically regulates extra-adrenal glucocorticoid synthesis in the intestine. J Exp Med 203, 2057-2062

19. Ahmed A, Schwaderer J, Hantusch A, Kolho KL & Brunner T (2019) Intestinal glucocorticoid synthesis enzymes in pediatric inflammatory bowel disease patients. Genes Immun 20, 566-576
20. Huang J, Jia R & Brunner T (2018) Local synthesis of immunosuppressive glucocorticoids in the intestinal epithelium regulates anti-viral immune responses. Cell Immunol 334, 1-10
21. Bayrer JR, Wang H, Nattiv R, Suzawa M, Escusa HS, Fletterick RJ, Klein OD, Moore DD & Ingraham HA (2018) LRH-1 mitigates intestinal inflammatory disease by maintaining epithelial homeostasis and cell survival. Nat Commun 9, 4055
22. Botrugno OA, Fayard E, Annicotte JS, Haby C, Brennan T, Wendling O, Tanaka T, Kodama T, Thomas W, Auwerx J & Schoonjans K (2004) Synergy between LRH-1 and beta-catenin induces G1 cyclin-mediated cell proliferation. Mol Cell 15, 499-509
23. Bayrer JR, Mukkamala S, Sablin EP, Webb P & Fletterick RJ (2015) Silencing LRH-1 in colon cancer cell lines impairs proliferation and alters gene expression programs. Proc Natl Acad Sci U S A 112, 2467-2472
24. Sidler D, Renzulli P, Schnoz C, Berger B, Schneider-Jakob S, Fluck C, Inderbitzin D, Corazza N, Candinas D & Brunner T (2011) Colon cancer cells produce immunoregulatory glucocorticoids. Oncogene 30, 2411-2419
25. Schoonjans K, Dubuquoy L, Mebis J, Fayard E, Wendling O, Haby C, Geboes K & Auwerx J (2005) Liver receptor homolog 1 contributes to intestinal tumor formation through effects on cell cycle and inflammation. Proc Natl Acad Sci U S A 102, 2058-2062
26. Ahmed A, Schmidt C & Brunner T (2019) Extra-Adrenal Glucocorticoid Synthesis in the Intestinal Mucosa: Between Immune Homeostasis and Immune Escape. Front Immunol 10, 1438
27. Volle DH, Duggavathi R, Magnier BC, Houten SM, Cummins CL, Lobaccaro J-MA, Verhoeven G, Schoonjans K & Auwerx J (2007) The small heterodimer partner is a gonadal gatekeeper of sexual maturation in male mice. Gene Dev 21, 303-315
28. Mombaerts P, Iacomini J, Johnson RS, Herrup K, Tonegawa S & Papaioannou VE (1992) RAG-1-deficient mice have no mature B and T lymphocytes. Cell 68, 869-877
29. Phan TS, Schink L, Mann J, Merk VM, Zwicky P, Mundt S, Simon D, Kulms D, Abraham S, Legler DF, Noti M & Brunner T (2021) Keratinocytes control skin immune homeostasis through de novo-synthesized glucocorticoids. Sci Adv 7, eabe0337
30. Neufert C, Becker C & Neurath MF (2007) An inducible mouse model of colon carcinogenesis for the analysis of sporadic and inflammation-driven tumor progression. Nat Protoc 2, 1998-2004
31. Horino J, Fujimoto M, Terabe F, Serada S, Takahashi T, Soma Y, Tanaka K, Chinen T, Yoshimura A, Nomura S, Kawase I, Hayashi N, Kishimoto T & Naka T (2008) Suppressor of cytokine signaling-1 ameliorates dextran sulfate sodium-induced colitis in mice. Int Immunol 20, 753-762
32. Noti M, Corazza N, Mueller C, Berger B & Brunner T (2010) TNF suppresses acute intestinal inflammation by inducing local glucocorticoid synthesis. J Exp Med 207, 1057-1066
33. Bode KJ, Mueller S, Schweinlin M, Metzger M & Brunner T (2019) A fast and simple fluorometric method to detect cell death in 3D intestinal organoids. Biotechniques 67, 23-28
34. Xue X & Shah YM (2013) In vitro Organoid Culture of Primary Mouse Colon Tumors. Jove-J Vis Exp 17, e50210
35. Canli O, Nicolas AM, Gupta J, Finkelmeier F, Goncharova O, Pesic M, Neumann T, Horst D, Lower M, Sahin U & Greten FR (2017) Myeloid Cell-Derived Reactive Oxygen Species Induce Epithelial Mutagenesis. Cancer Cell 32, 869-883
36. Michels BE, Mosa MH, Streibl BI, Zhan T, Menche C, Abou-El-Ardat K, Darvishi T, Czlonka E, Wagner S, Winter J, Medyouf H, Boutros M & Farin HF (2020) Pooled In Vitro and In Vivo CRISPR-Cas9 Screening Identifies Tumor Suppressors in Human Colon Organoids. Cell Stem Cell 26, 782-792 e787

37. Somers A, Jean JC, Sommer CA, Omari A, Ford CC, Mills JA, Ying L, Sommer AG, Jean JM, Smith BW, Lafyatis R, Demierre MF, Weiss DJ, French DL, Gadue P, Murphy GJ, Mostoslavsky G & Kotton DN (2010) Generation of transgene-free lung disease-specific human induced pluripotent stem cells using a single excisable lentiviral stem cell cassette. Stem Cells 28, 1728-1740
38. de Sousa e Melo FDE, Kurtova AV, Harnoss JM, Kljavin N, Hoeck JD, Hung J, Anderson JE, Storm EE, Modrusan Z, Koeppen H, Dijkgraaf GJP, Piskol R & de Sauvage FJ (2017) A distinct role for Lgr5(+) stem cells in primary and metastatic colon cancer. Nature 543, 676-680
39. Zhang C, Kolb A, Mattern J, Gassler N, Wenger T, Herzer K, Debatin KM, Buchler M, Friess H, Rittgen W, Edler L & Herr I (2006) Dexamethasone desensitizes hepatocellular and colorectal tumours toward cytotoxic therapy. Cancer Lett 242, 104-111
40. Brummelman J, Haftmann C, Nunez NG, Alvisi G, Mazza EMC, Becher B & Lugli E (2019) Development, application and computational analysis of high-dimensional fluorescent antibody panels for single-cell flow cytometry. Nat Protoc 14, 1946-1969
41. McInnes L, Healy J, Saul N & Grossberger L (2018) UMAP: uniform manifold approximation and projection. The Journal of Open Source Software 3, 861
42. Van Gassen S, Callebaut B, Van Helden MJ, Lambrecht BN, Demeester P, Dhaene T & Saeys Y (2015) FlowSOM: Using self-organizing maps for visualization and interpretation of cytometry data. Cytometry A 87, 636-645
43. Popivanova BK, Kostadinova FI, Furuichi K, Shamekh MM, Kondo T, Wada T, Egashira K & Mukaida N (2009) Blockade of a chemokine, CCL2, reduces chronic colitis-associated carcinogenesis in mice. Cancer Res 69, 7884-7892
44. Li Y, Choi M, Suino K, Kovach A, Daugherty J, Kliewer SA & Xu HE (2005) Structural and biochemical basis for selective repression of the orphan nuclear receptor liver receptor homolog 1 by small heterodimer partner. Proc Natl Acad Sci U S A 102, 9505-9510
45. Lu TT, Makishima M, Repa JJ, Schoonjans K, Kerr TA, Auwerx J & Mangelsdorf DJ (2000) Molecular basis for feedback regulation of bile acid synthesis by nuclear receptors. Mol Cell 6, 507-515
46. Ortlund EA, Lee Y, Solomon IH, Hager JM, Safi R, Choi Y, Guan Z, Tripathy A, Raetz CR, McDonnell DP, Moore DD & Redinbo MR (2005) Modulation of human nuclear receptor LRH-1 activity by phospholipids and SHP. Nat Struct Mol Biol 12, 357-363
47. Pan JH, Zhou H, Cooper L, Huang JL, Zhu SB, Zhao XX, Ding H, Pan YL & Rong LJ (2019) LAYN Is a Prognostic Biomarker and Correlated With Immune Infiltrates in Gastric and Colon Cancers. Frontiers in Immunology 10, 6
48. Bottcher JP, Bonavita E, Chakravarty P, Blees H, Cabeza-Cabrerizo M, Sammicheli S, Rogers NC, Sahai E, Zelenay S & Reis e Sousa C (2018) NK Cells Stimulate Recruitment of cDC1 into the Tumor Microenvironment Promoting Cancer Immune Control. Cell 172, 1022-1037 e1014
49. Gubin MM, Zhang X, Schuster H, Caron E, Ward JP, Noguchi T, Ivanova Y, Hundal J, Arthur CD, Krebber WJ, Mulder GE, Toebes M, Vesely MD, Lam SS, Korman AJ, Allison JP, Freeman GJ, Sharpe AH, Pearce EL, Schumacher TN, Aebersold R, Rammensee HG, Melief CJ, Mardis ER, Gillanders WE, Artyomov MN & Schreiber RD (2014) Checkpoint blockade cancer immunotherapy targets tumour-specific mutant antigens. Nature 515, 577-581
50. Ibata M, Takahashi T, Shimizu T, Inoue Y, Maeda S, Tashiro-Yamaji J, Okada M, Ueda K, Kubota T & Yoshida R (2011) Spontaneous rejection of intradermally transplanted non-engineered tumor cells by neutrophils and macrophages from syngeneic strains of mice. Microbiol Immunol 55, 726-735
51. Acharya N, Madi A, Zhang H, Klapholz M, Escobar G, Dulberg S, Christian E, Ferreira M, Dixon KO, Fell G, Tooley K, Mangani D, Xia J, Singer M, Bosenberg M, Neuberg D, Rozenblatt-Rosen O, Regev A, Kuchroo VK & Anderson AC (2020) Endogenous Glucocorticoid Signaling Regulates CD8(+) T Cell Differentiation and Development of Dysfunction in the Tumor Microenvironment. Immunity 53, 658-671 e656

52. Quatrini L, Vacca P, Tumino N, Besi F, Di Pace AL, Scordamaglia F, Martini S, Munari E, Mingari MC, Ugolini S & Moretta L (2021) Glucocorticoids and the cytokines IL-12, IL-15, and IL-18 present in the tumor microenvironment induce PD-1 expression on human natural killer cells. J Allergy Clin Immunol 147, 349-360
53. Fan ZW, Wang Z, Chen WR, Cao ZW & Li YX (2016) Association between the CYP11 family and six cancer types. Oncol Lett 12, 35-40
54. Noti M, Corazza N, Tuffin G, Schoonjans K & Brunner T (2010) Lipopolysaccharide induces intestinal glucocorticoid synthesis in a TNFalpha-dependent manner. FASEB J 24, 1340-1346

**Suplementary Material information**

**Suppl. Figure 1: Generation and characterization of intestine-specific Cyp11b1-deficient mice**

**Suppl. Figure 2: *In vitro* growth of tumor organoids**

**Suppl. Figure 3: Effect of dexamethasone treatment or *Cyp11b1* deletion on *in vivo* growth of s.c. transplanted tumors**

**Suppl. Figure 4: Characterization of tumor immune infiltrates**

**Suppl. Figure 5: Effect of NR5A2 and HSD11B2 expression on colorectal patient survival and immune marker expression**

**Suppl. Table 1: List of PCR and qRT-PCR primers**

**Figures Legends**

**Figure 1: Deletion of Lrh-1 in the intestinal epithelium attenuates colitis-associated colorectal cancer development.**

**A.** Scheme of azoxymethane (AOM)- and dextran sodium sulfate (DSS)-induced intestinal tumor induction. **B.** Weight loss curve of control (Lrh-1$^{fl/fl}$) mice and Lrh-1$^{IEC\ KO}$ mice after AOM treatment and during 3 cycles of DSS treatment. A representative experiment (n = 5 mice per group) of 3 repeats is shown (mean ± SD). **C.** Colonic tumor development (arrows) in control mice (Lrh-1$^{fl/fl}$) and Lrh-1$^{IEC\ KO}$ mice at day 56 following AOM/DSS treatment. **D, E.** Colonic tumor numbers (D) and tumor volume (E) of control and Lrh-1$^{IEC\ KO}$ mice (n = 7-8 per group). **F.** Numbers of colonic tumors stratified according to size. D-F, Mean ± SD of 3 independent experiments are shown. Unpaired student's T test, * $p< 0.05$, ** $p< 0.01$, ns not significant. Experiments were repeated 3 times and data were pooled.

**Figure 2: SHP suppresses LRH-1 transcriptional activity. A.** Murine mICcl2 cells were co-transfected with Myc/His-tagged β-Galactosidase (β-Gal) as control or SHP, and GFP-tagged LRH-1. Nuclear lysates were precipitated with $Ni^{2+}$-Sepharose. Proteins were detected using anti-Myc and anti-GFP antibodies. **B-D.** mICcl2 cells were transfected with an LRH-1 luciferase reporter (B), Cyp11a1 promoter reporter (C) or Cyp11b1 promoter reporter (D), mLRH-1 and increasing concentrations of mSHP expression plasmids. Relative luciferase units, normalized to β-galactosidase activity (rel. LU/bGal) were assessed. Mean values of triplicates ± SD are shown. One-way ANOVA with Turkey's multiple comparison **** $p<0.0001$. **E.** Detection of LRH-1 (*Nr5a2*), SHP (*Nr0b2*), *Cyp11a1* and *Cyp11b1* mRNA expression by RT-qPCR in liver, small intestine, large intestine, adrenal glands and isolated intestinal epithelial cells from wild type C57Bl/6 mice. Mean values of n=3 ± SD are shown. **F.** Expression of (LRH-1 (*Nr5a2*), cyclin E1 (*Ccne1*) and SHP (*Nr0b2*) along the crypt-villus axis. Epithelial cells from villus to crypt were differentially isolated and mRNA expression was analyzed by RT-qPCR. A typical experiment of n = 3 is shown.

**Figure 3: Effects of *Shp* deletion on LRH-1–regulated intestinal tumor development. A.** Detection of *Shp* (*Nr0b2*) in colonic tissue from control mice (Shp $^{+/+}$) and *Shp*-deficient mice (Shp $^{-/-}$) (n = 3 mice per group, mean ± SD). ND not detected. **B, C.** Expression of Lhr-1 (*Nr5a2*) and cyclin D1 (*Ccnd1*) along the crypt-villus axis. Epithelial cells from villus to crypt were differentially isolated from Shp $^{+/+}$ and Shp $^{-/-}$ mice, and mRNA expression was analyzed

by RT-qPCR. Mean values ± SD of 3 mice per group are shown. **D.** Weight loss curve of control (Shp $^{+/+}$) and Shp $^{-/-}$ after AOM/DSS treatment. Mean values ± SD of pooled 3 independent experiments are shown (n = 7-14 mice per group). **E.** Colonic tumor development (arrows) in control (Shp $^{+/+}$) and Shp $^{-/-}$ at day 64. **F, G.** Tumor numbers (F) and tumor volume (G) of Shp $^{+/+}$ and Shp $^{-/-}$ mice at day 56 and 64 (mean ± SD of n = 7 mice per group). **H.** Numbers of colonic tumors stratified according to size. Unpaired student's T test, * p< 0.05, ** p< 0.01, *** p< 0.001, **** p< 0.0001. **I.** Overall survival of Shp$^{+/+}$ and Shp$^{-/-}$ mice during AOM/DSS-induced colitis.

**Figure 4: Effect of Shp on acute colitis and intestinal glucocorticoid synthesis. A.** Scheme of acute colitis induction. **B.** Weight loss curve of Shp $^{+/+}$ and Shp $^{-/-}$ mice during acute DSS colitis (n = 3-6 mice per group and time point. Mean values ± SD). **C, D.** Colon shortening (C) and colitis score (D) of Shp $^{+/+}$ and Shp $^{-/-}$ mice at day 0 (UT), 5, 7 and 10 post DSS treatment (n = 3-6 mice per group and time point. Mean values ± SD). **E, F.** Colonic *Cyp11a1* (E) and *Cyp11b1* (F) mRNA expression in Shp $^{+/+}$ and Shp $^{-/-}$ mice at day 0 (UT), day 5, 7 and 10 post DSS treatment (n = 3-6 mice per group and time point. Mean values ± SD). **G.** *Ex vivo* colonic corticosterone synthesis (ng/g tissue) in Shp $^{+/+}$ and Shp $^{-/-}$ mice at day 0 (UT), day 5, 7 and 10 post DSS treatment (n = 3-6 mice per group and time point. Mean values ± SD). **H-J.** Colonic *Nr5a2* (H), *Tnf* (I) and *Il10* (J) mRNA expression in Shp $^{+/+}$ and Shp $^{-/-}$ mice at day 0 (UT), day 5 and 7 post DSS treatment (n = 3-6 mice per group and time point. Mean values ± SD). Unpaired student's T test (B-D, G), two-way ANOVA followed by Tukey's multiple comparison test (E, F, H-J), * p< 0.05, ** p< 0.01, *** p< 0.001, **** p< 0.0001, ns not significant. Typical experiments of n = 3 are shown.

**Figure 5: Role of colonic glucocorticoid synthesis in intestinal tumor development. A.** Scheme of AOM/DSS)-induced intestinal tumor induction. **B.** Weight loss curve of control (Cyp11b1 $^{fl/fl}$) and Cyp11b1$^{IEC\ KO}$ mice after AOM/DSS treatment. Mean values ± SD of pooled 3 independent experiments are shown (n = 6-13 mice per group). Unpaired student's T test, * p< 0.05. **C.** Colonic tumor development (arrows) in Cyp11b1 $^{fl/fl}$ and Cyp11b1$^{IEC\ KO}$ mice at day 35 and 56. **D.** Colonic tumor numbers in Cyp11b1 $^{fl/fl}$ and Cyp11b1$^{IEC\ KO}$ mice at day 35 and 56 (n = 6-7 mice per group and time point). Unpaired student's T test, * p< 0.05. **E.** Detection of immune checkpoints (*Cd279*, *Cd274, Cd152*), M2 macrophage marker (*Arg1*), and cytokines (*Tnf, IL6, Tgfb, Il10*) in Cyp11b1 $^{fl/fl}$ and Cyp11b1$^{IEC\ KO}$ tumors at day 48 (n = 4-5 mice). Unpaired student's T test, p values are indicated.

**Figure 6: Role of Lrh-1 and Shp in growth regulation of transplanted tumor organoids.** **A.** Scheme of tumor organoid development and s.c. transplantation into C57Bl/6 wild type recipients. **B.** *In vivo* growth of transplanted control (Lrh-$1^{fl/fl}$) and Lrh-$1^{IEC\ KO}$ tumor organoids after s.c. transplantation into C57Bl/6 wild type mice. Mean values ± SD of n = 12 mice per group are shown. Experiments were repeated twice. **C.** Growth of individual tumors summarized in B. **D.** Weight of isolated tumors from the experiment shown in B. **E.** Examples of tumors isolated at day 24 post transplantation. **F.** Histology of Lrh-$1^{fl/fl}$ and Lrh-$1^{IEC\ KO}$ tumors at day 24 post transplantation. Inlay shows magnification. Scale bars: overview 300 µm, inlay 150 µm. **G.** *In vivo* growth of transplanted control Shp $^{+/+}$ and Shp $^{-/-}$ tumor organoids after s.c. transplantation into C57Bl/6 wild type mice. Mean values ± SD of n = 12 mice per group are shown. Experiments were repeated twice. **H.** Growth of individual tumors summarized in G. **I.** Weight of isolated tumors from the experiment shown in G. **J.** Examples of tumors isolated at day 24 post transplantation. **K.** Histology of control Shp $^{+/+}$ and Shp $^{-/-}$ tumors at day 24 post transplantation. Inlay shows magnification. Scale bars: overview 300 µm, inlay 150 µm. Mean ± SD are shown. Unpaired student's T test, * $p< 0.05$, ** $p< 0.01$, *** $p< 0.001$, **** $p< 0.0001$.

**Figure 7: Role of tumor glucocorticoid synthesis in immune evasion of transplanted tumor organoids.** Control (Cyp11b1 $^{fl/fl}$) and Cyp11b1 $^{IEC\ KO}$ tumor organoids were transplanted into immunocompetent C57Bl/6 wild type recipients (WT) (A) or lymphopenic *Rag1*-deficient mice (RAG KO) (B). **A, B.** Tumor growth of transplanted tumors. Mean values ± SD of n = 12-26 mice per group are shown. **C, E.** Mean values ± SD of tumor weight of isolated Cyp11b1 $^{fl/fl}$ and Cyp11b1 $^{IEC\ KO}$ tumors at day 12 post transplantation into wild type recipient mice (C) (n = 26 mice per group) or *Rag1*-deficient mice (E) (n = 12 mice per group). Data points of tumors from the same recipient mice have been connected by lines. Unpaired student's T test. ns not significant, * $p< 0.05$, ** $p< 0.01$, *** $p< 0.001$, **** $p< 0.0001$. Experiments have been repeated 4 times (A) and 2 times (B). **D, F.** Examples of tumors isolated at day 12 post transplantation. **G-I.** High dimensional flow cytometry analysis of tumor infiltrating immune cells from control (Cyp11b1 $^{fl/fl}$)- or *Cyp11b1*-deficient (Cyp11b1 $^{IEC\ KO}$) tumors at day 9 post transplantation. Data represent combined samples with n = 5 mice per group. **G.** UMAP plot with manually annotated FlowSOM cell clusters of 100'000 cells combined from all tumors (10'000 cells randomly sampled per tumor). **H.** Heatmap with lineage marker expressions (columns) over the manually annotated FlowSOM cell clusters (rows). **I.** Total cell numbers of indicated cell clusters presented as box plots showing the 25$^{th}$ to 75$^{th}$ percentiles with whiskers indicating the range to the smallest and largest data point until the 1.5x IQR. Dots in box plots represent individual mice. Box plots with median values,

and lower and upper quartiles are shown DN cDCs, double-negative conventional dendritic cells; moDCs, monocyte-derived dendritic cells; lineage, pDCs, plasmacytoid DCs.

**Figure 8: Survival curves of colon cancer patients with high or low expression of *CYP11A1*, *HSD11B1* and *NR0B2*. A.** Colon cancer patients were stratified into groups of the highest or lowest quartile expression of the genes *CYP11A1*, *HSD11B1* or *NR0B2* (SHP), and survival was analyzed (95 patients per group). Statistical differences (p values) are indicated. **B.** Individual tumor from the highest or lowest quartile expression of *CYP11A1*, *HSD11B1* and *NR0B2* were analyzed for the expression of genes related to immunoregulatory cytokines (*TGFB1*, *IL10*), immune checkpoints (*CD279* (PD-1, *CD274* (PD1-1L), *CD152* (CTLA-4)), and M2-like macrophage markers (*LAYN*, *CCR4, ARG1*). The data were derived from 379 colon adenocarcinoma (COAD) samples from the TCGA database using upper (high) quartile (n = 95) vs. lower (low) quartile (n = 95) expression of the given gene (*CYP11A1, HSD11B1* or *NR0B2*) to form the groups analyzed. Kaplan-Meier survival plots comparing the higher quartile *versus* lower quartile groups defined by expression of each gene indicated. The expression levels of immune genes are shown as the log RPKM - Reads per kilo base per million mapped reads. Box plots with median values, and lower and upper quartiles, and minima and maxima are shown. All markers show significant differences (** p< .01) between high and low *CYP11A1*, *HSD11B1* and *NR0B2* expressors.

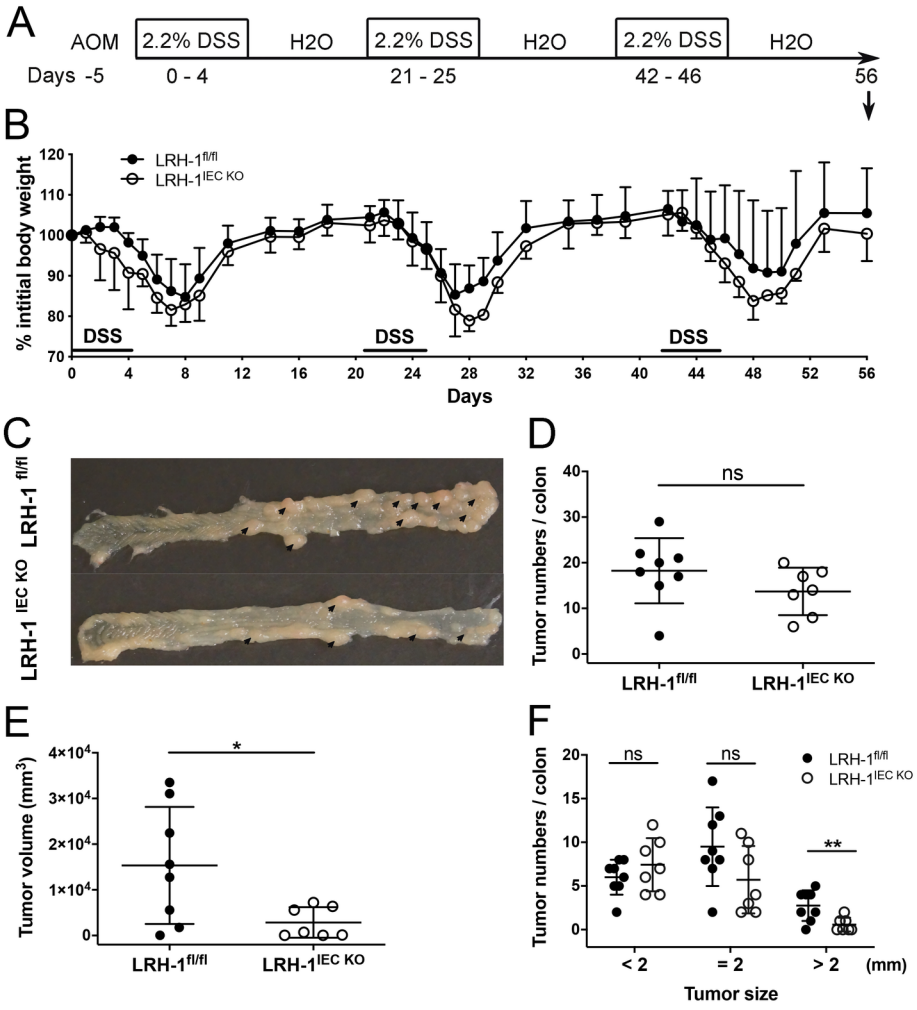


MOL2_13414_Figure 1.tif

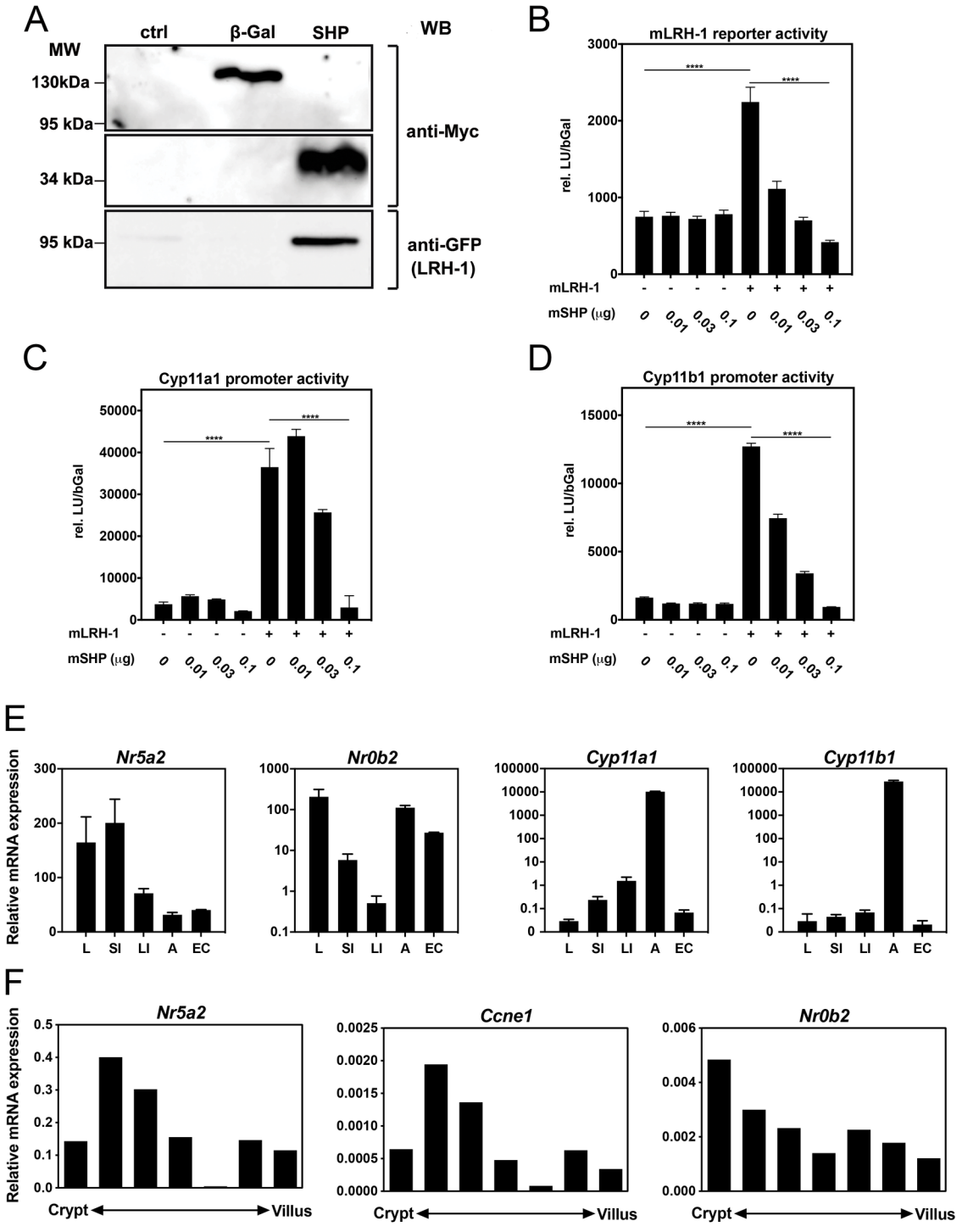


MOL2_13414_Figure 2.tif

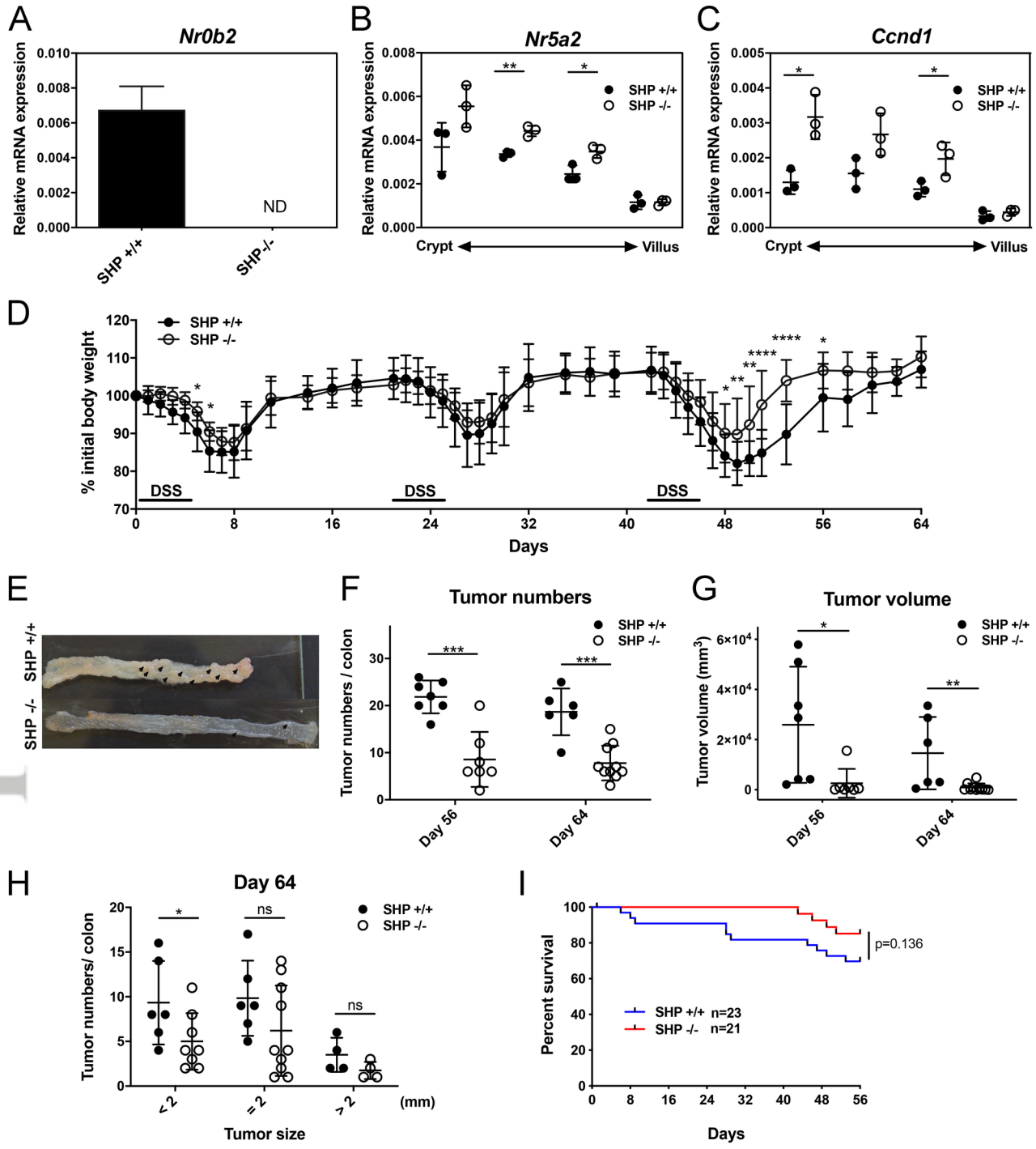


MOL2_13414_Figure 3.tif

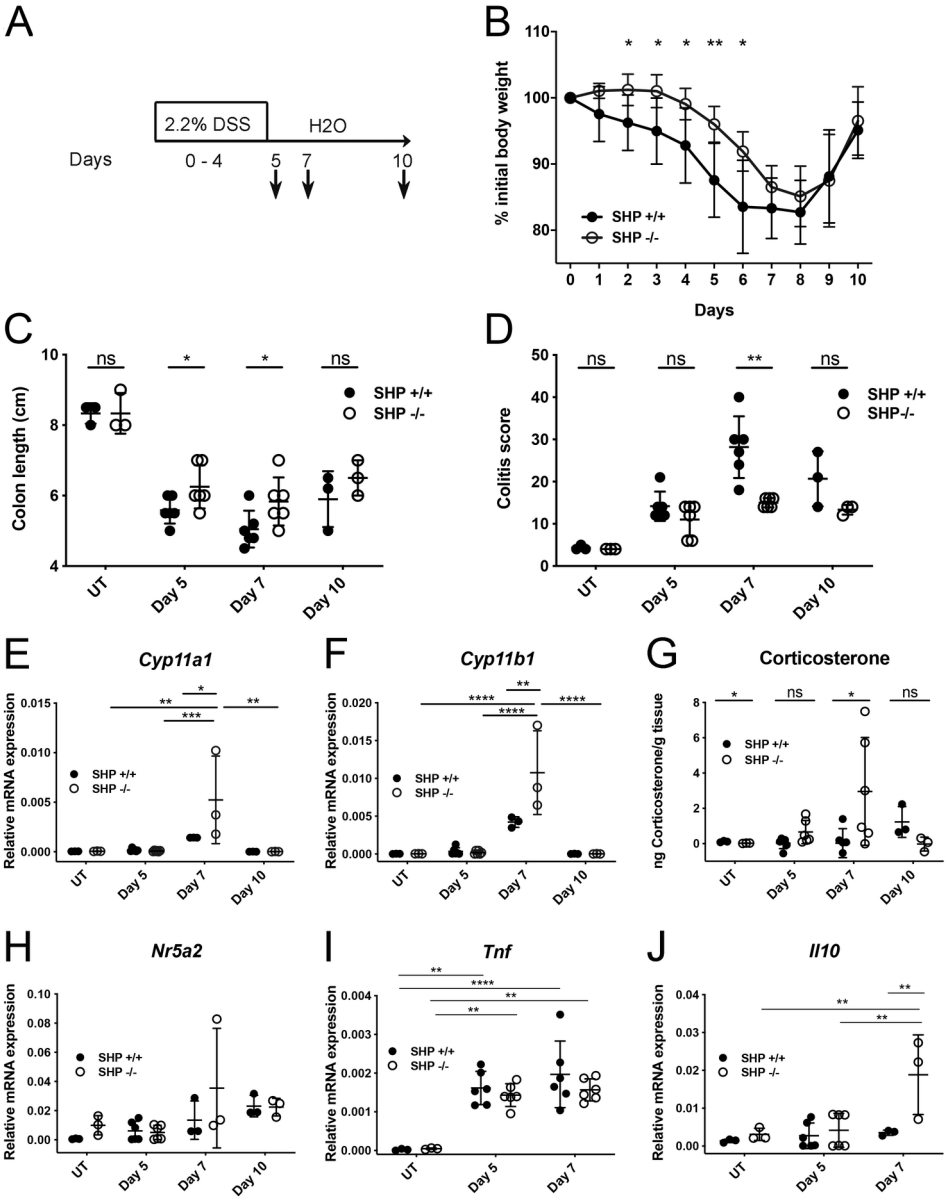


MOL2_13414_Figure 4.tif

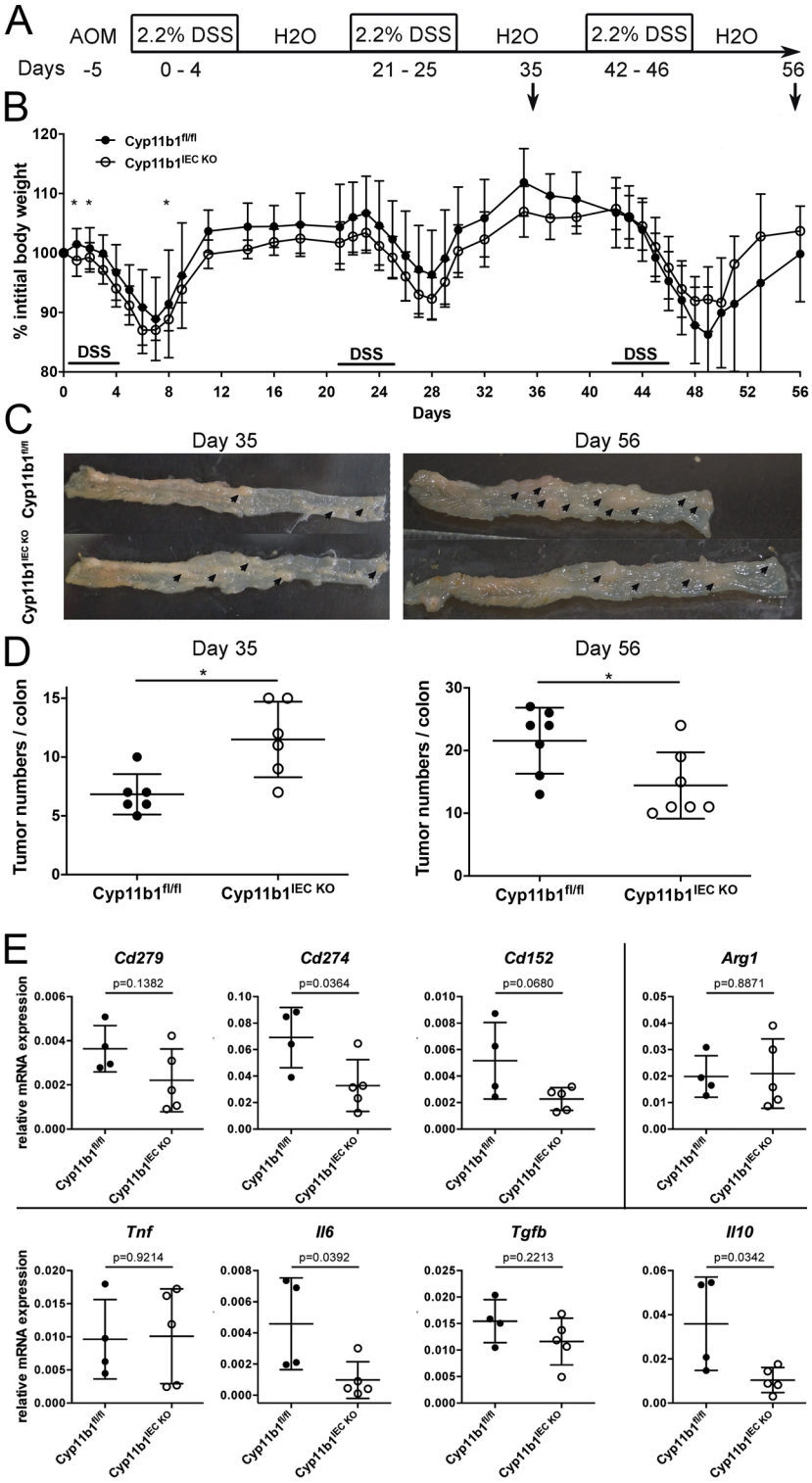


MOL2_13414_Figure 5.tif

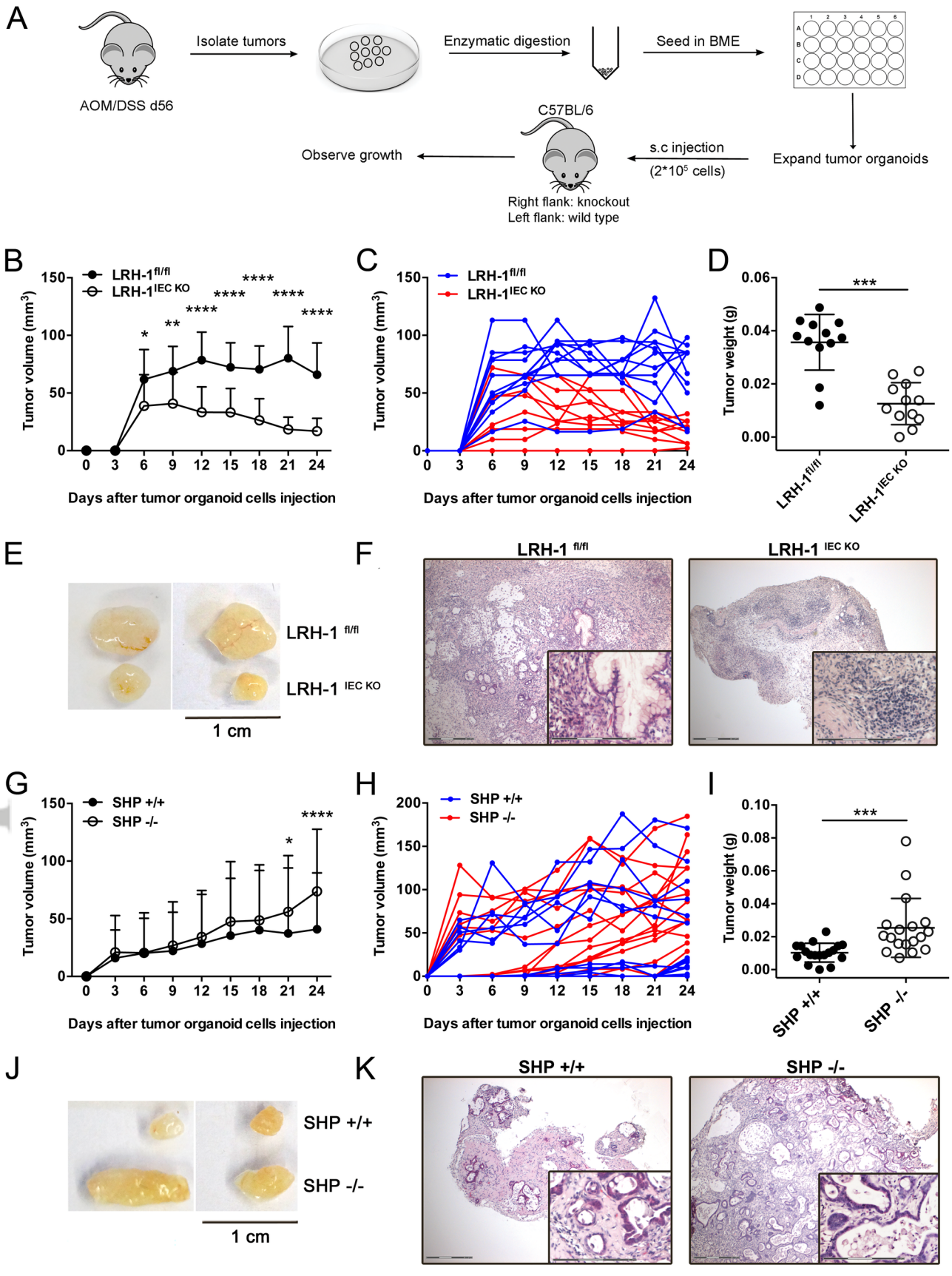


MOL2_13414_Figure 6.tif

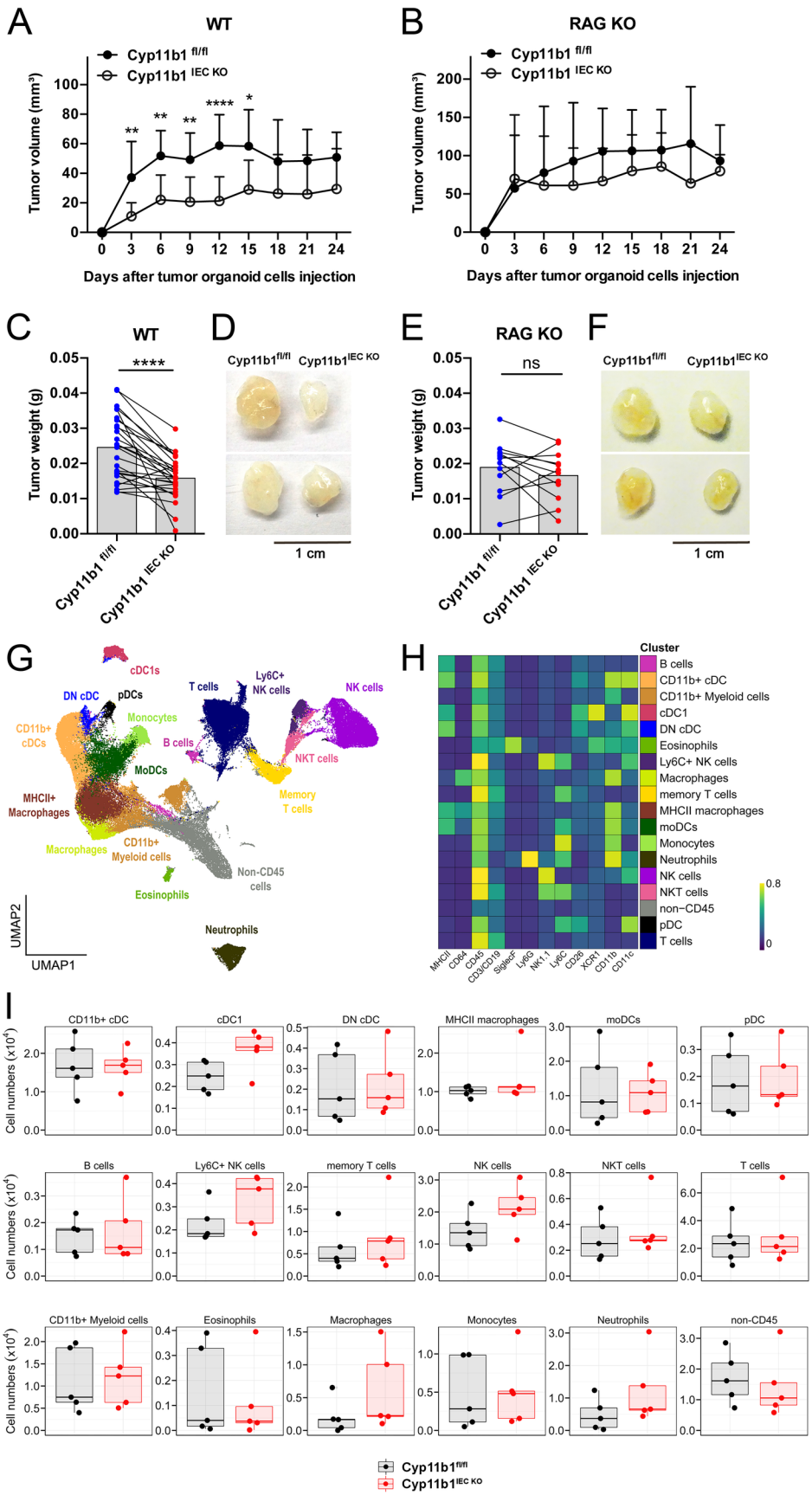


MOL2_13414_Figure 7.tif

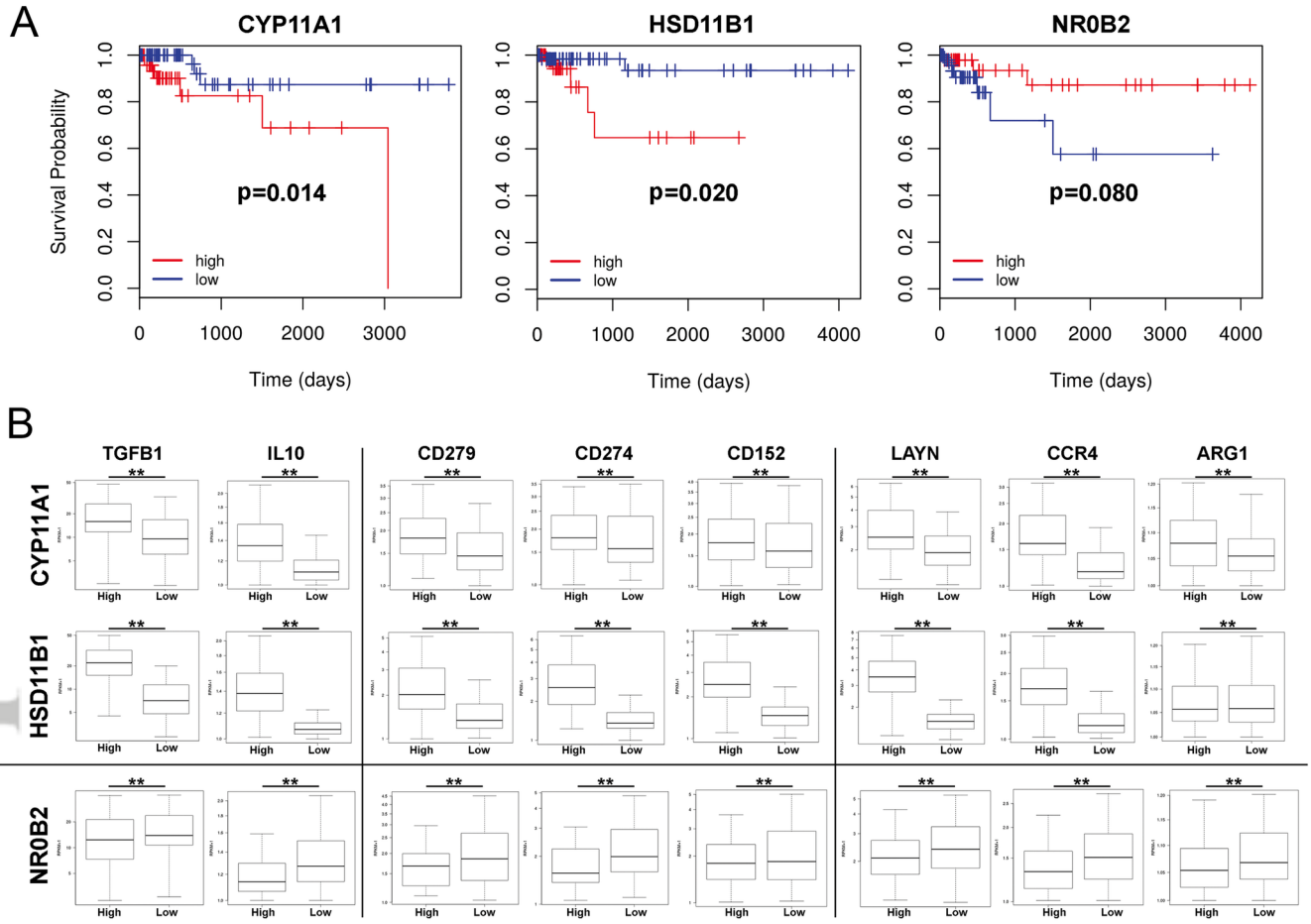


MOL2_13414_Figure 8.tif